Transworld Research Network
37/661 (2), Fort P.O., Trivandrum-695 023, Kerala, India

Recent Res. Devel. Sound & Vibration, 2(2004): 115-150 ISBN: 81-7895-119-3

7 Nonlinear dynamics of the Helmholtz Oscillator

Juan A. Almendral, Jesús Seoane and Miguel A. F. Sanjuán
Nonlinear Dynamics and Chaos Theory Group, Departamento de Matemáticas y Física Aplicadas y Ciencias de la Naturaleza, Universidad Rey Juan Carlos, Tulipán, s/n, 28933 Móstoles, Madrid, Spain

Abstract

The Helmholtz Oscillator is the simplest asymmetrical nonlinear oscillator, containing a quadratic nonlinearity. Its nonlinear dynamics is reviewed here including an exhaustive description of the formulation of the model and a thorough analysis of the solutions for the undamped and unforced case, and the construction of the separatrix map. The effect of the parametric and quasiperiodic driving is also analized. A special attention is devoted when the linear damping is considered, obtaining the corresponding symmetries and conditions for the complete integrability of the system. Finally the effect of using a nonlinear damping term is considered, showing analytical and computational results.

Correspondence/Reprint request: Dr. Miguel A. F. Sanjuán, Nonlinear Dynamics and Chaos Theory Group, Departamento de Matemáticas y Física Aplicadas y Ciencias de la Naturaleza, Universidad Rey Juan Carlos, Tulipán, s/n, 28933 Móstoles Madrid, Spain. E-mail: msanjuan@escet.urjc.es

I. Introduction

Oscillations and waves are ubiquitous in nature and are easily modelled through the help of differential equations. The general equation for the one-dimensional oscillatory motion of a unit mass particle, can be easily understood using a mechanical analogy. Assume that the particle moves in a force field which is generated by the potential $V(x)$, then the general equation of motion may be written as

$$\ddot{x} + \frac{dV}{dx} = 0. \tag{1}$$

Stated the problem this way, different oscillators may be obtained, depending on the potential $V(x)$ acting on the particle. Assuming $V(x)$ to be a polynomial function in x, very few cases with analytical solutions have been studied. Among them the Duffing oscillator, with a nonlinear term of fourth order, and the Helmholtz oscillator [1] when the cubic term is used. Obviously higher order terms may be considered, which in general lead to rather complicated mathematical solutions. These are the nonlinear versions of the oscillator given by Eq. (1). If only the quadratic term is taken into account obviously the harmonic oscillator is derived. Another simple case with a non-polynomial potential $V(x) = -\cos x$ is the pendulum equation. It is important to remark that from all these four model equations complete analytical solutions are known in closed form. While circular functions are the solutions of the harmonic oscillator, Jacobian elliptic functions are in general, the solutions of the nonlinear oscillators considered here.

The study of an oscillator of this kind is worthwhile in spite of its apparent simplicity, because many physical problems of application may be reduced to the analysis of this simple nonlinear oscillator. The dynamics of the Helmholtz oscillator mimics the dynamics of certain prestressed structures, the capsize of a ship [2] and the nonlinear dynamics of a drop in a time-periodic flow [3] or in a time-periodic electric field [4]. It appears also in relation to the randomization of solitary-like waves in boundary-layer flows [5], in the three-wave interaction, also referred as to resonant triads [6] and in connection to steady reductions of some perturbative KdV equations governing nonlinear waves and solitons [7-9].

If it is included a linear damping δ and a periodic forcing F in Eq. (1), it is obtained

$$\ddot{x} + \delta\dot{x} + \frac{dV}{dx} = F\cos(\omega t), \tag{2}$$

where the inclusion of damping and forcing on the system bestows rather different dynamical behavior as compared with the case without them.

Even though an analysis in absence of damping has been accomplished for the pendulum equation [10, 11], as well as for the Duffing oscillator [12]; very few results are known for the Helmholtz oscillator. Perhaps this can be explained because it might be thought that the cubic oscillator and the quadratic oscillator keep many things in common, though this is not so. In spite of that, when damping is considered, this system has received some attention by different authors [1, 2, 13].

Damping in certain applied systems play an important role, since it may be used to suppress large amplitude oscillations or various instabilities, and it can be also used as a control mechanism. The role of nonlinear dissipation in double-well Duffing oscillators received some attention by [14, 15], where a single nonlinear damping term proportional to the power of the velocity is used and one of the conclusions is that nonlinear damping terms affects especially the onset of the period-doubling route to chaos.

Numerous physical phenomena of oscillatory nature appearing in different disciplines present the ability to escape from a potential well, and are described by the Helmholtz oscillator. This nonlinear oscillator has a simple mechanical interpretation, since it describes the motion of a particle of unit mass in the single cubic potential $V(x) = x^2/2 - x^3/3$ sinusoidally driven, and is considered as a prototype for escape phenomena. When a linear dissipative force is introduced, its equation of motion is

$$\ddot{x} + \delta\dot{x} + x - x^2 = F\sin(\omega t), \tag{3}$$

where δ represents the damping level, F the forcing amplitude and ω the frequency of the external perturbation.

Extensive numerical and analytical studies on different aspects related to this simple nonlinear oscillator can be found in [2, 16-21] and analytical work related to the escape from the potential well was examined by [22-24]. Besides, an experimental apparatus was constructed to mimic the equation and is described in [25]. A control method of the homoclinic bifurcation applied to the nonlinear dynamics of the Helmholtz Oscillator is developed in Ref. [26] by Lenci and Rega. When a simple linear damping term is introduced in the dynamics of the nonlinear oscillator, it implies that a complete integrability of the system is not allowed. However in the unforced case, certain conditions are fulfilled in such a way that the damped oscillator is completely integrable [27]. The effect of using nonlinear damping terms on the universal escape oscillator is considered in Ref. [28] by Sanjuán. For a general review on nonlinearly damped oscillators see Ref. [29]. Even though some authors [17, 25] mention the possible interesting role played by considering nonlinear damping terms, the fact is that they only contemplated linear damping terms. This paper is organized as follows. An analysis and description of the model equation is carried out in Section II. The analysis is rather complete, including the analytical solutions for the undamped and unforced case and the construction of the separatrix map. The nonlinear Helmholtz Oscillator perturbed parametrically and quasiperiodically is analized in section III. Section IV is devoted to the analysis of the oscillator with linear damping and its integrability and corresponding symmetries. A thorough analysis of the effect of nonlinear damping on the dynamics of the oscillator is done in section V. And finally some concluding remarks are described in section VI.

II. Analysis and description of the model

A. Introduction

The equation of motion of a particle of unit mass which undergoes a periodic forcing in a cubic single-well potential with damping, reads

$$\ddot{x} + \delta\dot{x} + \alpha x - \beta x^2 = F\cos(\omega t), \tag{4}$$

where δ, α, β, F and ω are positive constants.

The Eq. (4) can be seen from the point of view of the Hamiltonian and Lagrangian formalism, see [8, 30-33]. The original idea goes back to the article of Bateman [34], where he introduces the transformation in the Lagrangian formulation for the linear damped harmonic oscillator, while he was trying to prove that a linear dissipative system can be derived from a variational principle. A generalization of the transformation used in [30, 33] can be found in [35], where a linear oscillator with time-dependent friction and frequency is considered. Later, Havas [36] studies the range of application of the Lagrangian and Hamiltonian formalism. This was also used by Denman [37] in order to study the Hamilton-Jacobi equation and to analyze dissipative systems for its possible treatment in quantum mechanics.

Concerning Hamiltonian formalism for nonlinear oscillators with dissipation terms, Denman [37] gives the general expression for the Lagrangian and the Hamiltonian. This is developed later by Steeb [38] for a class of dissipative dynamical systems with limit cycle and chaotic behavior, and the explicit Lagrange and Hamilton functions are given.

The particular case given by Eq. (4) is derived from a time-dependent Hamiltonian and Lagrangian of the following form

$$H(p,x,t) = \frac{1}{2}p^2 e^{-\delta t} + e^{\delta t}V(x,t), \tag{5}$$

$$L(\dot{x},x,t) = e^{\delta t}\left[\frac{1}{2}\dot{x}^2 - V(x,t)\right], \tag{6}$$

where $V(x,t)$ is the following generalized potential for the whole system

$$V(x,t) = \frac{\alpha x^2}{2} - \frac{\beta x^3}{3} - Fx\cos(\omega t). \tag{7}$$

In this section, it is considered that $\delta = 0$ (i.e., there is no damping). Hence, the equation to analyze is

$$\ddot{x} + \alpha x - \beta x^2 = F\cos(\omega t), \tag{8}$$

and therefore, Eqs. (5, 6) become

$$H(p,x,t) = \frac{1}{2}p^2 + V(x,t), \tag{9}$$

$$L(\dot{x},x,t) = \frac{1}{2}\dot{x}^2 - V(x,t), \tag{10}$$

which will be useful for the computation of the homoclinic orbit and for the construction of the separatrix map. This construction will be analyzed in a subsequent section.

B. Single-well potential

When $F = 0$, the equation of a conservative oscillator is obtained. This oscillator may be understood as a particle which is situated in a single potential well $V(x)$ defined as

$$V(x) = \frac{\alpha x^2}{2} - \frac{\beta x^3}{3}. \tag{11}$$

One important feature of this system, easily seen in Fig. 1, is that according to the initial condition and the energy of the particle, the orbits may be bounded or unbounded. When the value of the energy $E_{\min} = 0 \leq E \leq E_{\max} = \frac{\alpha^3}{6\beta^2}$, then there exist possibilities of bounded motions, hence oscillations, while for $E > E_{\max}$ the motion of the particle is unbounded, that is, the particle escapes to infinity.

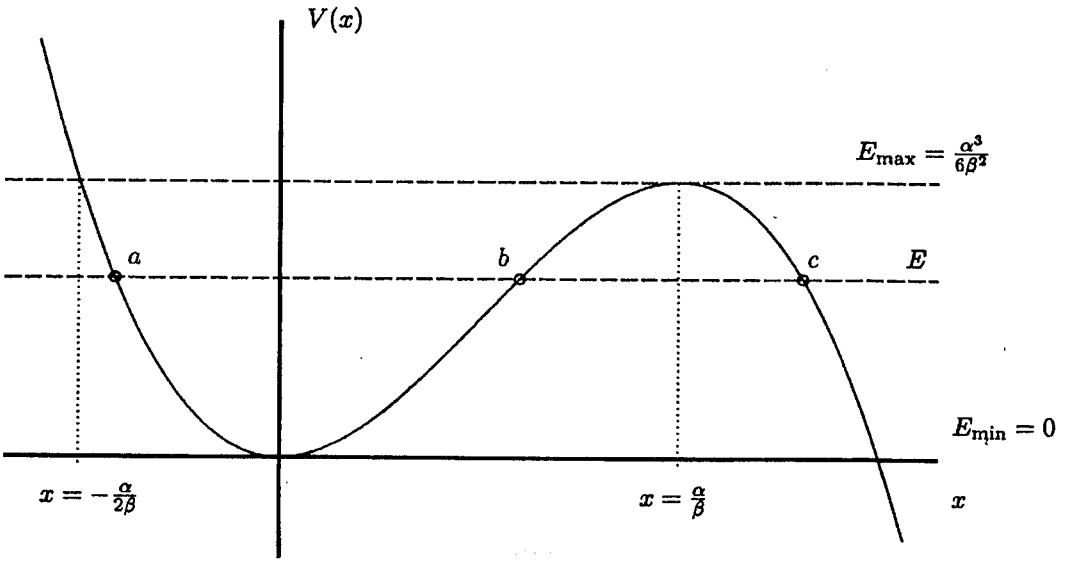

Figure 1. Potential energy associated to the Helmholtz oscillator, which may be seen as the simplest potential with an escape. Notice that the potential has been chosen to be $V(x) = \frac{\alpha}{2}x^2 - \frac{\beta}{3}x^3$, because in this way α and β are positive constants. The orbits will be bounded only when $-\frac{\alpha}{2\beta} < x < \frac{\alpha}{\beta}$ and $0 < E < E_{\max}$. For instance, the bounded orbit with energy E is comprised within $[a, b]$. If $x > c$ then the orbit is unbounded.

When the particle has energy E in the range $[E_{\min}, E_{\max}]$, then the cubic equation $E - V(x) = 0$ provides three real roots a, b and c, $(a < b < c)$, which represent physically the *turning points*, that is, the points where the velocity of the particle changes sign. These roots verifies the following relationships which will be important for further results

$$a + b + c = \frac{3\alpha}{2\beta}, \quad ab + bc + ac = 0, \quad abc = -\frac{3E}{\beta}. \tag{12}$$

and their general expressions are

$$a = \frac{\alpha}{2\beta} + (-1-m)\frac{\lambda}{3}, \quad b = \frac{\alpha}{2\beta} + (2m-1)\frac{\lambda}{3}, \quad c = \frac{\alpha}{2\beta} + (2-m)\frac{\lambda}{3}, \tag{13}$$

where to obtain the former results, the following parameters are used

$$m = \frac{b-a}{c-a} \quad , \quad \lambda = c-a. \tag{14}$$

If it is defined also

$$\Delta^2 = 1 - m + m^2, \tag{15}$$

then, from the Eqs. (12), it is derived that

$$\frac{\alpha}{2\beta} = \frac{\lambda\Delta}{3}; \tag{16}$$

a useful expression which allows to express the values of the roots in terms only of the parameter m

$$\begin{aligned} a &= \frac{\alpha}{2\beta} + (-1-m)\frac{\alpha}{2\beta\Delta}, \\ b &= \frac{\alpha}{2\beta} + (2m-1)\frac{\alpha}{2\beta\Delta}, \\ c &= \frac{\alpha}{2\beta} + (2-m)\frac{\alpha}{2\beta\Delta}. \end{aligned} \tag{17}$$

C. General exact solution

Now the equation of motion Eq. (4) can be solved exactly in the conservative case, i.e., in the absence of damping and periodic forcing. Hence, the analytical solutions of the periodic orbits inside the single well will be derived.

The conservation of energy can be used to set the problem in terms of the three roots of $E - V(x) = 0$ in the following way

$$\frac{\dot{x}^2}{2} = \frac{\beta}{3}(x-a)(x-b)(x-c). \tag{18}$$

The terms can be rearranged into

$$\frac{dx}{dt} = \sqrt{\frac{2\beta}{3}}\sqrt{(x-a)(x-b)(x-c)}, \tag{19}$$

and now after a simple integration of the above equation it is achieved the following result

$$t - t_0 = \sqrt{\frac{3}{2\beta}}\int_a^x \frac{dx}{\sqrt{(x-a)(x-b)(x-c)}}, \tag{20}$$

where it is assumed that the particle lies in $x = a$ for the initial time t_0. Now assume the following change of variable

$$x = a + (b - a)\sin^2\theta, \tag{21}$$

and introducing this result into Eq. (20) it is obtained that

$$t - t_0 = \sqrt{\frac{6}{\beta(c-a)}}\int_0^{\phi}\frac{d\theta}{\sqrt{1 - m\sin^2\theta}}. \tag{22}$$

The solution of the integral in the right-hand side is given by the *sine amplitude* of a Jacobian elliptic function [39] from where it is deduced that

$$\sqrt{\frac{\beta(c-a)}{6}}(t - t_0) = \int_0^{\phi}\frac{d\theta}{\sqrt{1 - m\sin^2\theta}} = \mathrm{sn}^{-1}(\sin\phi; m), \tag{23}$$

where ϕ is the *elliptic amplitude* and m is the *elliptic parameter*. There is a lot of confusion in the literature about the use of the *elliptic parameter* m and the *elliptic modulus* k, which are related by the expression $k^2 = m$. The notation of [39] is followed here, where $\mathrm{sn}(u; k)$ represents the sine amplitude when the elliptic modulus is used, while $\mathrm{sn}(u; m)$ when the elliptic parameter is used. For simplicity, the elliptic parameter is used throughout.

Thus, from the last equation is inferred

$$\sin\phi = \mathrm{sn}\left(\sqrt{\frac{\beta(c-a)}{6}}(t - t_0); m\right), \tag{24}$$

and if the change of variable used before is taken into account, the following solution is obtained

$$x(t) = a + (b - a)\mathrm{sn}^2\left(\sqrt{\frac{\beta(c-a)}{6}}(t - t_0); m\right), \tag{25}$$

which is the general solution for all the periodic orbits lying within the single well. Note that all orbits are labelled by the elliptic parameter m. This parameter m which ranges from $0 \leq m \leq 1$ is in fact the same previously defined in Eq. (14) in relation to the turning points of motion in the potential well. It labels the energy of each periodic orbit inside the potential well.

D. Period of the orbits

It is also interesting to calculate the period of each and everyone of the orbits inside the potential well. For this purpose the following integral has to be worked out

$$T(m) = 2\sqrt{\frac{3}{2\beta}}\int_b^c \frac{dx}{\sqrt{(x-a)(x-b)(x-c)}} = \sqrt{\frac{6}{\beta(c-a)}}\int_0^{\frac{\pi}{2}} \frac{d\theta}{\sqrt{1-m\sin^2\theta}}. \tag{26}$$

The last integral represents exactly the *complete elliptic integral of the first kind* $K(m)$ [39], so that

$$T(m) = \sqrt{\frac{24}{\beta(c-a)}}K(m). \tag{27}$$

For orbits whose energy is very small in absolute terms, i.e., $m \to 0$, the complete elliptic integral of first kind $K(m) \to \frac{\pi}{2}$ and then the period becomes $T \to \sqrt{\frac{4}{\alpha}}\pi$. This is obviously the period for the linear oscillations around the elliptic fixed point (0, 0). However for values of the energy close to the separatrix, which means $m \to 1$, the complete elliptic integral of the first kind diverges logarithmically in this way

$$K(m) \approx \frac{1}{2}\ln\left(\frac{16}{1-m}\right), \tag{28}$$

and this means that the period also diverges logarithmically for values of m close to unity

$$T(m) = \frac{2}{\sqrt{\alpha}}\ln\left(\frac{16}{1-m}\right). \tag{29}$$

E. Equation of the separatrix

From the general solution obtained before is rather easy to derive the equation of the separatrix orbit. In fact the separatrix orbit is the orbit with energy corresponding to the parameter $m = 1$ and which possesses a period infinity. The sine amplitude of the Jacobian elliptic function has two natural limiting functions depending on the limit values of m. These limiting functions are $\mathrm{sn}(u; m) \to \sin u$, for $m \to 0$ and $\mathrm{sn}(u; m) \to \tanh u$, for $m \to 1$.

Moreover, if $m = 1$, then $\Delta = 1$, $a = -\frac{\alpha}{2\beta}$ and $b = c = \frac{\alpha}{\beta}$ from Eq. (15) and Eqs. (17). Hence, if it is assumed that $t_0 = 0$ to simplify, the separatrix is given by

$$x_{sx}(t) = \frac{3\alpha}{2\beta}\left[\frac{2}{3} - \cosh^{-2}\left(\sqrt{\frac{\alpha}{4}}t\right)\right], \tag{30}$$

$$y_{sx}(t) = \frac{3}{2}\sqrt{\frac{\alpha^3}{\beta^2}}\frac{\sinh\left(\sqrt{\frac{\alpha}{4}}t\right)}{\cosh^3\left(\sqrt{\frac{\alpha}{4}}t\right)}, \tag{31}$$

which has a fish-shaped form. Actually, it is easy to check that $y_{sx}(t)$ and $x_{sx}(t)$ are related this way

$$y_{sx}^2 = \frac{2}{3}\beta\left(x_{sx} - \frac{\alpha}{\beta}\right)^2\left(x_{sx} + \frac{\alpha}{2\beta}\right). \tag{32}$$

The bounded motions lie in the interior of the separatrix, while the unbounded motions lie outside. In this case the separatrix corresponds to a *homoclinic orbit*, since the orbit connects the hyperbolic fixed point $(\frac{\alpha}{\beta}, 0)$ to itself.

F. Stochastic layer

Once the Helmholtz oscillator has been analyzed, it is interesting the study on how the orbits behave in the proximity of the separatrix when a periodic forcing is applied.

The time-dependent Hamiltonian in Eq. (6) can be used, as it was explained in the introduction of this section, to study the Helmholtz oscillator with a periodic forcing. This time-dependent Hamiltonian can be seen as the sum of a time-independent Hamiltonian

$$H_0(x,p) = \frac{1}{2}p^2 + \frac{\alpha}{2}x^2 - \frac{\beta}{3}x^3 \tag{33}$$

and a time-dependent Hamiltonian

$$H_1(x,t) = -Fx\cos(\omega t), \tag{34}$$

that is, the Hamiltonian $H(p,x,t)$ can be written this way

$$H(p,x,t) = H_0(x,p) + H_1(x,t) \tag{35}$$

The former Hamiltonian allows analyzing the effect of the forcing by means of an area preserving map, which is called the *whisker map* or the *separatrix map*. This map measures the energy and phase change of a trajectory close to the separatrix for each period of the motion [40].

In order to construct this map it is needed to evaluate the change of the Hamiltonian H_0. The total derivative of H_0 is the following

$$\frac{dH_0}{dt} = \{H_0, H\} = \{H_0, H_1\} = -\frac{\partial H_0}{\partial \dot{x}}\frac{\partial H_1}{\partial x} = F\dot{x}\cos(\omega t), \tag{36}$$

where $\{\}$ is the Poisson bracket.

Since our main interest is discussing the motion of the particle when its energy is close to the separatrix, it is assumed that F is small enough to consider that H_1 is a small perturbation. Then, it is close to the separatrix where big effects in the dynamics of the particle may be expected. The effect of a small perturbation on the orbits of small energy is negligible.

The method to obtain the separatrix map, when H_1 is consider to be a small perturbation, is standard [40]. The first step is the computation of the energy ΔE. This

energy accounts for the amount of the energy which an orbit close to the separatrix needs to accomplish a complete cycle, and is given through the integration of Eq. (36)

$$\Delta E = F \int_{\Delta t} \dot{x} \cos(\omega t) dt, \tag{37}$$

where $\Delta t = T/2 = \pi/\omega$. Notice that this integral signals the border of the stochastic layer.

This energy is usually written in the following way to be evaluated around the separatrix

$$\Delta E_n = F \int_{t_n - \frac{T}{2}}^{t_n + \frac{T}{2}} \dot{x} \cos(\omega t) dt \approx F \int_{-\infty}^{+\infty} y_{sx} \cos\left[\omega \left(t + t_n\right)\right] dt. \tag{38}$$

From the third equality in Eqs. (12) and Eqs. (13) a relationship between the energy E and the parameter m is found. Expanding around $m = 1$ up to second order, it is obtained the following expression $8E \approx (1 - m)^2$. This approximation is used later to determine the separatrix map and its corresponding stochastic layer.

The change of the phase is given by $\Delta\phi = \omega T$. The expression for the energy relationship found before in terms of m, when m is close to 1, suggests that the period of the orbits close to the separatrix behaves like

$$T(m) \approx \frac{1}{\sqrt{\alpha}} \ln\left(\frac{32}{E}\right). \tag{39}$$

In this manner the change of energy E and phase ϕ from the period n to the period $n+1$ is given by the separatrix mapping [11]

$$E_{n+1} = E_n + \Delta E_n, \tag{40}$$

$$\phi_{n+1} = \phi_n + \omega T_{n+1}, \tag{41}$$

where the variables (E, ϕ) are to be understood as a canonical pair. This map contains in principle the essential dynamics in the region close to the separatrix. Thus, the separatrix map is given by

$$E_{n+1} = E_n + \frac{6\pi\omega^2}{\beta} \frac{F \sin\phi_n}{\sinh\left(\frac{\pi\omega}{\sqrt{\alpha}}\right)}, \tag{42}$$

$$\phi_{n+1} = \phi_n + \frac{\omega}{\sqrt{\alpha}} \ln\left(\frac{32}{E_{n+1}}\right). \tag{43}$$

Another way of measuring the instability is through the calculation of the following parameter K defined as [11]

$$K = \left| \frac{\delta\phi_{n+1}}{\delta\phi_n} - 1 \right|, \tag{44}$$

from which as a by-product the stochastic layer width is achieved. It supplies the information about how a small phase interval is stretched. The measure of the local instability is given by $K \geq 1$, because close to the separatrix a small change in frequency may cause a big effect in phase. The stochastic layer width is given by the value

$$E \approx \frac{6\pi F\omega^3}{\sqrt{\alpha}\beta \sinh\left(\sqrt{\frac{\pi^2}{\alpha}}\omega\right)}, \tag{45}$$

which corresponds to the width of the region close to the separatrix where it is likely to expect chaotic motions.

III. Parametric and quasiperiodic perturbations

A. Introduction

Two of the main reasons to study the periodically driven nonlinear oscillators are the rich dynamic behavior observed in them and the enormous applications of these nonlinear oscillators in order to model oscillatory and complex phenomena in all branches of science [41]. Besides periodically driven nonlinear oscillators, also quasiperiodically and parametrically driven nonlinear oscillators are worthy of analysis [42-52].

The Melnikov theory is the suitable analytical tool to ascertain the critical parameter values from which it is expected a system to show chaotic behavior of the Smale-horseshoe type [53]. In spite of the power of the method in predicting the chaotic threshold, it is important to note, however, that in practice the true observed threshold, results to be above the predicted one and this is mainly due to its intrinsic perturbative nature [52, 54, 55].

A complete study of the the homoclinic bifurcation sets of the quasiperiodically forced Duffing oscillator can be found in Ref. [42], and a similar situation for the case of the parametrically driven Duffing oscillator is found in Ref. [56] .

The method used in both cases is basically the same. First, the original equation is written as a set of two coupled first order differential equations in suspended form, then the Melnikov technique is applied, evaluating the Melnikov function which depends upon the different parameters of the original nonlinear oscillator. Finally a criterion for the occurrence of chaos of the Smale-horseshoe type is established for the damping coefficient δ, in such a way that whenever this coefficient is less than a critical value δ_c, then transverse intersections of the stable and the unstable manifolds do occur, and the attendant chaotic dynamics is expected.

Then, the corresponding homoclinic bifurcation sets are constructed in the parameter space, namely $(\delta, f_1, ..., f_n, \omega_1, ..., \omega_n)$, where δ is the damping coefficient, $\{f_i\}_{i=1,...,n}$ are the respective parameters of the forcings and $\{\omega_i\}_{i=1,...,n}$ are the corresponding associated frequencies. This homoclinic bifurcation set is given by the

surface which is obtained through the mathematical condition provided by the Melnikov method. For the quasiperiodically forced oscillator, $\{f_i\}_{i=1,...,n}$ represent the competing quasiperiodical external forces, while in the parametrically driven oscillator, they represent competition between the parametric forcings and the external forcing.

The method to represent these bifurcations curves in the $(\omega_1, ..., \omega_n)$ space for a chosen set of values of $(\delta, f_1, ..., f_n)$ consists on defining n functions, say $\{X_i(\omega_1)\}_{i=1,...,n}$, in such a way that the mathematical condition obtained for the threshold of chaotic behavior can be rewritten basically as

$$-k + \sum_{i=1}^{n} f_i X_i(\omega_i) = 0. \tag{46}$$

Since this equation is linear in f_i and $X_i(\omega_i)$, it can be regarded as a surface in the parameter space. Then, using the properties of the functions $X_i(\omega_i)$, it is possible to redraw the bifurcation curves in the $(\omega_1, ..., \omega_n)$ space, from the curves in the $(X_1, ..., X_n)$ space. Finally, the complete homoclinic bifurcation sets of the corresponding oscillator are drawn in the $(X_1, ..., X_n)$ space and in the $(\omega_1, ..., \omega_n)$ space for the different cases in the $(\delta, f_1, ..., f_n)$ space. More details concerning this construction can be found in [42, 56].

The main difference of both analysis lies in the different nature of the functions $X_i(\omega_i)$. While in the case of the parametrically driven oscillator these functions possess different maxima, in the quasiperiodically forced oscillator these functions possess their maxima at the same frequency. This results in different bifurcations sets in the $(\omega_1, ..., \omega_n)$ space, along with some additional subcases for the second case, as is shown in [56].

B. The parametrically driven Helmholtz oscillator

The equation of motion for the parametrically driven Helmholtz oscillator, with a periodic external forcing and a parametric modulation acting both in the linear and nonlinear dynamical variable, is given by

$$\ddot{x} + \delta\dot{x} + \alpha[1 + \gamma_\alpha \sin(\omega_\alpha t)]x - \beta[1 + \gamma_\beta \sin(\omega_\beta t)]x^2 = F \sin(\Omega t), \tag{47}$$

where α, β, δ, F, ω_α, ω_β and Ω are positive constants and, γ_α and γ_β are parameters which values are in the interval [0, 1].

For the unperturbed system, i.e., when $\gamma_\alpha = \gamma_\beta = \delta = F = 0$, we obtain the conservative Helmholtz oscillator. Its hamiltonian can be written as

$$H(\dot{x}, x) = \frac{\dot{x}^2}{2} + \frac{\alpha x^2}{2} - \frac{\beta x^3}{3}. \tag{48}$$

whose homoclinic orbit is given by the Eqs. (30, 31).

The presence of the perturbations added to the oscillator causes the stable and unstable manifolds to be destroyed, giving rise to the possibility of chaotic solutions. We

are interested in the calculation of the Melnikov distance $\Delta(t_0)$ for the case in which all the perturbations are considered. A transformation of $\delta \to \varepsilon\delta$, $\gamma_\alpha \to \varepsilon\gamma_\alpha$, $\gamma_\beta \to \varepsilon\gamma_\beta$ and $F \to \varepsilon F$ is done in order to apply the ε first-order perturbation scheme of the Melnikov theory.

Hence, the Eq. (47) may be written as

$$\dot{x} = y, \tag{49}$$

$$\dot{y} = -\alpha x + \beta x^2 + \varepsilon\{F\sin(\Omega t) - \alpha\gamma_\alpha x_{sx}(t)\sin(\omega_\alpha t) + \beta\gamma_\beta x_{sx}^2(t)\sin(\omega_\beta t) - \delta y_{sx}(t)\}, \tag{50}$$

and the Melnikov distance is evaluated as

$$\Delta(t_0) = \int_{-\infty}^{+\infty} y_{sx}(t-t_0)\quad \{F\sin(\Omega t) - \alpha\gamma_\alpha x_{sx}(t-t_0)\sin(\omega_\alpha t) + \beta\gamma_\beta x_{sx}^2(t-t_0)\sin(\omega_\beta t) - \delta y_{sx}(t-t_0)\}\, dt, \tag{51}$$

which can be written in three parts, $\Delta_0(t_0)$, $\Delta_{\gamma_\alpha}(t_0)$ and $\Delta_{\gamma_\beta}(t_0)$. The first term corresponds to the case in which there is only external forcing, while the second and the third terms are the contribution of the parametric forcing in α and β respectively.

Then, the computation of the Melnikov distance is $\Delta(t_0) = \Delta_0(t_0) + \Delta_{\gamma_\alpha}(t_0) + \Delta_{\gamma_\beta}(t_0)$, where

$$\Delta_0(t_0) = \frac{6\pi}{\beta}\frac{\Omega^2 F\cos(\Omega t_0)}{\sinh(\pi\Omega/\sqrt{\alpha})} - \frac{6\alpha^{5/2}}{5\beta^2}\delta, \tag{52}$$

$$\Delta_{\gamma_\alpha}(t_0) = \frac{3\pi\alpha^2}{\beta^2}\frac{\omega_\alpha^2\gamma_\alpha\cos(\omega_\alpha t_0)}{\sinh(\pi\omega_\alpha/\sqrt{\alpha})}\left(-1+\frac{\omega_\alpha^2}{\alpha}\right), \tag{53}$$

$$\Delta_{\gamma_\beta}(t_0) = \frac{3\pi\alpha^2}{\beta^2}\frac{\omega_\beta^2\gamma_\beta\cos(\omega_\beta t_0)}{\sinh(\pi\omega_\beta/\sqrt{\alpha})}\left(\frac{4}{5}-\frac{\omega_\beta^2}{\alpha}+\frac{\omega_\beta^4}{5\alpha^2}\right). \tag{54}$$

The condition for transverse intersection and chaotic separatrix motion holds, when $\Delta(t_0)$ changes sign at some t_0 [53]. This criterion for the appearance of chaos can be finally written, for the case in which $\alpha = \beta = 1$, in the form

$$\delta \le \delta_c = \frac{5\pi F\Omega^2}{\sinh(\pi\Omega)} + \frac{\pi\gamma_\alpha\omega_\alpha^2}{2\sinh(\pi\omega_\alpha)}(-5+5\omega_\alpha^2) + \frac{\pi\gamma_\beta\omega_\beta^2}{2\sinh(\pi\omega_\beta)}(4-5\omega_\beta^2+\omega_\beta^4). \tag{55}$$

Hence, if we define

$$f_1 = 5\pi F \qquad X_1(\Omega) = \frac{\Omega^2}{\sinh(\pi\Omega)}, \tag{56}$$

$$f_2 = \frac{\pi}{2}\gamma_\alpha \qquad X_2(\omega_\alpha) = \frac{\omega_\alpha^2}{\sinh(\pi\omega_\alpha)}(-5 + 5\omega_\alpha^2), \tag{57}$$

$$f_3 = \frac{\pi}{2}\gamma_\beta \qquad X_3(\omega_\beta) = \frac{\omega_\beta^2}{\sinh(\pi\omega_\beta)}(4 - 5\omega_\beta^2 + \omega_\beta^4), \tag{58}$$

the Eq. (55) can be rewritten in the form

$$-\delta + f_1 X_1(\Omega) + f_2 X_2(\omega_\alpha) + f_3 X_3(\omega_\beta) = 0. \tag{59}$$

The function $X_1(\Omega)$ has a maximum at $\Omega = 0.61$, $X_2(\omega_\alpha)$at $\omega_\alpha = 1.65$ and $X_3(\omega_\beta)$ at $\omega_\beta = 0.41$. This can be observed in Fig. 2, which represents the plots of $X_1(\Omega)$, $X_2(\omega_\alpha)$ and $X_3(\omega_\beta)$, showing their respective maxima at different frequencies.

The remaining analysis of the homoclinic bifurcation sets for the parametrically driven Helmholtz oscillator is then qualitatively the same as the one exposed by [56]. This is due to the similitude of the problem and also to the qualitative nature of the analysis carried out there.

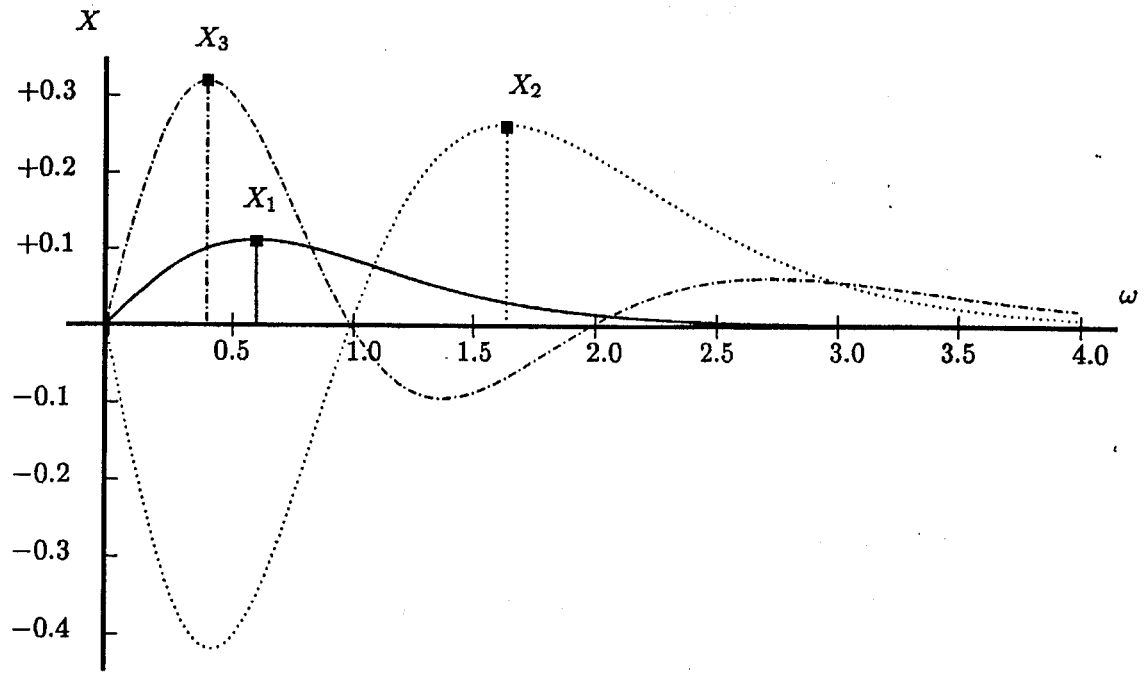

Figure 2. Plots of the auxiliary functions $X_1(\Omega)$, $X_2(\omega_\alpha)$ and $X_3(\omega_\beta)$. The most important feature is that the $X_i(\omega)$ functions have maxima at different frequencies.

C. The quasiperiodically forced Helmholtz oscillator

Now we consider that, instead of the parametric drive on the dynamic variable, we add another external periodic forcing. Hence, the equation of motion of the quasiperiodically forced Helmholtz oscillator is the following

$$\ddot{x} + \delta\dot{x} + \alpha x - \beta x^2 = F_1 \sin(\Omega_1 t) + F_2 \sin(\Omega_2 t), \tag{60}$$

which, after applying the first order perturbation theory, can be written as

$$\dot{x} = y, \tag{61}$$

$$\dot{y} = -\alpha x + \beta x^2 + \varepsilon\{F_1 \sin(\Omega_1 t) + F_2 \sin(\Omega_2 t) - \delta y_{sx}(t)\}. \tag{62}$$

Then, the Melnikov distance is evaluated similarly to the parametrically driven case,

$$\begin{aligned}\Delta(t_0) &= \int_{-\infty}^{+\infty} y_{sx}(t-t_0)\{F_1 \sin(\Omega_1 t) + F_2 \sin(\Omega_2 t) - \delta y_{sx}(t-t_0)\}\, dt, \\ &= \frac{6\pi}{\beta}\frac{\Omega_1^2 F_1 \cos(\Omega_1 t_0)}{\sinh(\pi\Omega_1/\sqrt{\alpha})} + \frac{6\pi}{\beta}\frac{\Omega_2^2 F_2 \cos(\Omega_2 t_0)}{\sinh(\pi\Omega_2/\sqrt{\alpha})} - \frac{6\alpha^{5/2}}{5\beta^2}\delta,\end{aligned} \tag{63}$$

where y_{sx} is given by the Eq. (31).

Therefore, for the case in which $\alpha = \beta = 1$, the expression for the bifurcation set obtained through the Melnikov analysis is given by

$$-\delta + 5\pi F_1 \Omega_1^2 \mathrm{csch}(\pi\Omega_2) + 5\pi F_2 \Omega_2^2 \mathrm{csch}(\pi\Omega_2) = 0, \tag{64}$$

which is qualitatively identical to the expression found in [42].

Notice that this implies that the homoclinic bifurcations curves are identical. The Eq. (64) can be written as

$$-\delta + f_1 X_1(\Omega_1) + f_2 X_2(\Omega_2) = 0. \tag{65}$$

If we define

$$f_1 = 5\pi F_1 \qquad X_1(\Omega_1) = \frac{\Omega_1^2}{\sinh(\pi\Omega_1)}, \tag{66}$$

$$f_2 = 5\pi F_2 \qquad X_2(\Omega_2) = \frac{\Omega_2^2}{\sinh(\pi\Omega_2)}, \tag{67}$$

then, the functions $X_1(\Omega_1)$ and $X_2(\Omega_2)$ have their maxima at the same frequency $\Omega_1 = \Omega_2 = 0.61$.

IV. Analysis of the oscillator with linear damping: Integrability and symmetries

A. Introduction

A way of studying the Helmholtz oscillator is by means of computational methods. Nowadays, the use of a computer allows calculating good approximations to the solution of many problems. However, analytical methods give important information about the dynamical behavior of the system. Chaotic aspects of certain dynamical systems are better understood when the analytical structure is known [57]. Actually, the analytical structure comprises information about the integrability of the model, and this is useful to assure whether chaos is possible or not. This link between integrability and chaotic motion has been analyzed for several models, for instance, the Lorenz model [58] or the Hénon-Heiles Hamiltonian [59].

The *Lie theory for differential equations* is a powerful method to study analytically a dynamical system. Actually, this theory was developed originally to study differential equations. Different techniques developed to solve certain types of equations (i.e., separable or exact equations) are regarded in this theory as special cases of a general integration method.

Lie theory allows determining when the equation is integrable and its symmetry group. Basically, a symmetry group of a differential equation is a group which transforms solutions to other solutions of the equation. In the case of an ordinary differential equation, this is useful to integrate it, since invariance under a symmetry implies that the order of the equation can be reduced by one. Hence, for a second order equation, as the Helmholtz oscillator, two symmetries are needed to integrate it and to write the solution in terms of known functions.

However, besides the exact formulas and expressions for a generic oscillator, it is important to remark that new insights and intuitions can be derived from its study, which may help to understand the dynamics of other similar problems.

In this section the Helmholtz oscillator in Eq. (4) is analyzed in the absence of the periodic forcing, i.e., when $F = 0$. Then, the equation of motion of a particle of unit mass reads

$$\ddot{x} + \delta\dot{x} + \alpha x - \beta x^2 = 0. \tag{68}$$

To investigate the integrability of this equation the *Lie theory of differential equations* will be used [60, 61]. However, it should be noticed that the integrability of a differential equation can be also analyzed by means of the Kowalewski's asymptotic method (also called the Painlevé singularity structure analysis) and the same result is achieved. For example, in [43, 62] the Duffing oscillator is analyzed in this manner. Nevertheless, the Lie theory is used in this work because this approach, in addition to give information about when the equation is integrable, allows reducing the problem to canonical variables which eases integrating the equation in a more general and natural way.

It can be seen in [60, 61] that in order to find the symmetry group G admitted by a differential equation with infinitesimal operator

$$X = \eta(t,x)\frac{\partial}{\partial x} + \xi(t,x)\frac{\partial}{\partial t}, \tag{69}$$

it is needed to find an infinitesimal operator X_{+2} such that

$$X_{+2}(\ddot{x} + \delta\dot{x} + \alpha x - \beta x^2) = 0. \tag{70}$$

The operator X_{+2} is

$$X_{+2} = \xi(t,x)\frac{\partial}{\partial t} + \eta(t,x)\frac{\partial}{\partial x} + A(t,x,\dot{x})\frac{\partial}{\partial \dot{x}} + B(t,x,\dot{x},\ddot{x})\frac{\partial}{\partial \ddot{x}}, \tag{71}$$

where $A(t,x,\dot{x})$ and $B(t,x,\dot{x},\ddot{x})$ are defined as follows

$$A(t,x,\dot{x}) = \eta_t + \dot{x}(\eta_x - \xi_t) - \dot{x}^2\xi_x, \tag{72}$$

$$B(t,x,\dot{x},\ddot{x}) = \eta_{tt} + \dot{x}(2\eta_{xt} - \xi_{tt}) + \dot{x}^2(\eta_{xx} - 2\xi_{tx}) - \dot{x}^3\xi_{xx} + \ddot{x}(\eta_x - 2\xi_t - 3\dot{x}\xi_x), \tag{73}$$

with the usual notation $\omega_z \equiv \frac{\partial\omega}{\partial z}$.

All $\xi(t,x)$ and $\eta(t,x)$ such that verify Eq. (70) generate infinitesimal operators X as in Eq. (69) which comprise the symmetries of the differential equation. Also, it is known that one symmetry can be used to reduce by one the order of a differential equation. Thus, to integrate a second order differential equation two symmetries are needed. Hence, the Helmholtz oscillator will be integrated only if $\xi(t,x)$ and $\eta(t,x)$ are such that they generate two linearly independent infinitesimal operators.

B. Condition of integrability

Following the procedure to determine the symmetries of a differential equation mentioned in the former section, Eq. (70) reads

$$X_{+2}(\ddot{x} + \delta\dot{x} + \alpha x - \beta x^2) = \eta(\alpha - 2\beta x) + \delta\left(\eta_t + \dot{x}(\eta_x - \xi_t) - \dot{x}^2\xi_x\right) + \eta_{tt}$$
$$+\dot{x}(2\eta_{xt} - \xi_{tt}) + \dot{x}^2(\eta_{xx} - 2\xi_{xt}) - \dot{x}^3\xi_{xx} - \left(\delta\dot{x} + \alpha x - \beta x^2\right)(\eta_x - 2\xi_t - 3\dot{x}\xi_x). \tag{74}$$

This is a polynomial of third degree in $[\dot{x}]$ which is zero if and only if the coefficients of every monomial is zero

$$[\dot{x}^3] \;:\; \xi_{xx} = 0, \tag{75}$$

$$[\dot{x}^2] \;:\; \eta_{xx} - 2\xi_{xt} + 2\delta\xi_x = 0, \tag{76}$$

$$[\dot{x}] \;:\; 2\eta_{xt} - \xi_{tt} + 3\xi_x(\alpha x - \beta x^2) + \delta\xi_t = 0, \tag{77}$$

$$[1] \;:\; \eta(\alpha - 2\beta x) + \delta\eta_t + \eta_{tt} - (\eta_x - 2\xi_t)(\alpha x - \beta x^2) = 0. \tag{78}$$

From the condition in Eq. (75) it is plain that $\xi(x,t) = f(t) + k(t)x$, and this result in Eq. (76) implies that $\eta(x,t) = (k'(t) - \delta k(t))x^2 + xg(t) + h(t)$. If both results are used in Eq. (77) it is deduced that

$$4\left(k''-\delta k'\right)x+2g'-\left(f''+k''x\right)+3k\left(\alpha x-\beta x^2\right)+\delta\left(f'+k'x\right)=0. \tag{79}$$

This is a polynomial of second degree in $[x]$ which is zero if and only if the three following equations are verified

$$[x^2]\ :\ 3\beta k=0, \tag{80}$$

$$[x]\ :\ k''+3\delta k'-3\alpha k=0, \tag{81}$$

$$[1]\ :\ 4k''-f''+\delta f'+2g'=0. \tag{82}$$

These three equations imply that $k=0$, hence $\xi(x,t)=f(t)$ and $\eta(x,t)=xg(t)+h(t)$, with the following relation between $f(t)$ and $g(t)$

$$\delta f'+2g'-f''=0. \tag{83}$$

According to these results the condition in Eq. (78) is reduced to

$$(gx+h)(\alpha-2\beta x)+\delta\left(xg'+h'\right)+xg''+h''+\left(\alpha x-\beta x^2\right)\left(-g+2f'\right)=0. \tag{84}$$

This is a polynomial of second degree in $[x]$ which is zero if and only if the following three equations are verified

$$[x^2]\ :\ g+2f'=0, \tag{85}$$

$$[x]\ :\ 2\alpha f'+\delta g'+g''-2\beta h=0, \tag{86}$$

$$[1]\ :\ \alpha h+\delta h'+h''=0. \tag{87}$$

The conditions in Eq. (83) and Eq. (85) imply that $g=Ae^{\frac{1}{5}\delta t}$ with A a constant. When this result is used in Eq. (86) it is obtained that $h=\frac{1}{2\beta}\left(\frac{6}{25}\delta^2-\alpha\right)g$. And finally, this result in Eq. (87) means that $\frac{1}{2\beta}\left(\frac{6}{25}\delta^2+\alpha\right)\left(\frac{6}{25}\delta^2-\alpha\right)g=0$. But, since it is supposed that $\alpha>0$and so $\frac{6}{25}\delta^2+\alpha>0$, there are only two options to verify all conditions.

The first one is when $g=0$. In this case $h=0$ and $f=$ *constant* and this means that $\eta=0$ and $\xi=$ *constant.* Hence, only one infinitesimal operator is obtained, namely $X=\vartheta_t$, and as a consequence, the differential equation is partially integrable.

The second option in order to get two symmetries is when

$$\alpha=\frac{6}{25}\delta^2. \tag{88}$$

In this case $h = 0$ and $g = Ae^{\frac{1}{5}\delta t}$, which implies that $f = B - \frac{5}{2\delta}Ae^{\frac{1}{5}\delta t}$ and consequently $\xi = B - \frac{5}{2\delta}Ae^{\frac{1}{5}\delta t}$ and $\eta = Axe^{\frac{\delta}{5}t}$. Therefore, two infinitesimal generators are found, namely

$$X_1 = \frac{\partial}{\partial t}, \tag{89}$$

$$X_2 = -\frac{5}{2\delta}e^{\frac{1}{5}\delta t}\frac{\partial}{\partial t} + xe^{\frac{1}{5}\delta t}\frac{\partial}{\partial x}. \tag{90}$$

In conclusion, only when it is verified that $\alpha = \frac{6}{25}\delta^2$ the Helmholtz oscillator with damping is completely integrable. Therefore, there is a lot of information about the oscillator in this particular case, but there should be noticed that the information applies just for a 2-dimensional manifold in the parameter space $\{\delta, \alpha, \beta, \gamma\}$. When $\alpha \neq \frac{6}{25}\delta^2$ the oscillator is only partially integrable and there is no way to write down the solution in terms of known functions.

C. Reduction to canonical variables

The infinitesimal generators X_1 and X_2 defined in Eqs. (89) are a 2-dimensional algebra L_2 since $[X_1, X_2] = \frac{\delta}{5}X_2$, where [] is a *commutator*, called Lie bracket, defined in the following manner $[X_1, X_2] = X_1X_2 - X_2X_1$. This *Lie algebra* can be classified according to its structural properties [60] as type III because $[X_1, X_2] = \frac{\delta}{5}X_2 \neq 0$ and $X_1 \vee X_2 = xe^{\frac{1}{5}\delta t} \neq 0$, where $\vee$ is a *pseudoscalar product* defined this way $X_1 \vee X_2 = \xi_1\eta_2 - \xi_2\eta_1$, if $X_i = \xi_i\partial_1 + \eta_i\partial_2$ for $i = 1, 2$. Actually, L_2 is the algebra of the homothety transformations of the real line $\mathbb{R}$, where X_1 is a homothety operator and X_2 is a translation operator.

Then, it is known that there exists a pair of variables w and z, called *canonical variables*, which linearizes the action of the group G on $\mathbb{R}$ and reduce the algebra L_2 to $X_1 = w\partial_w + z\partial_z$ and $X_2 = \partial_z$.

Let w and z be

$$w \equiv Axe^{\frac{2}{5}\delta t}, \tag{91}$$

$$z \equiv Be^{-\frac{1}{5}\delta t}, \tag{92}$$

where A and B are constants, then

$$X_1 = \frac{2\delta}{5}\omega\frac{\partial}{\partial\omega} - \frac{\delta}{5}z\frac{\partial}{\partial z}, \tag{93}$$

$$X_2 = \frac{B}{2}\frac{\partial}{\partial z}. \tag{94}$$

Although it is not the canonical form, there is no need to introduce more changes because it is simple enough to reduce the Helmholtz oscillator to an easily integrable equation.

From the definitions stated in Eqs. (91) the following result is obtained

$$w'' = \frac{d}{dz}\left(\frac{dw}{dz}\right) = \frac{25A}{B^2\delta^2} e^{\frac{1}{5}\delta t} \frac{d}{dt}\left[\left(\dot{x} + \frac{2}{5}\delta x\right) e^{\frac{3}{5}\delta t}\right]$$
$$= \frac{25A}{B^2\delta^2} e^{\frac{4}{5}\delta t}\left(\ddot{x} + \delta\dot{x} + \frac{6\delta^2}{25}x\right) = \frac{25\beta}{\delta^2 AB^2} w^2. \tag{95}$$

Therefore, if A and B are chosen such that

$$AB^2 = \frac{25\beta}{6\delta^2}, \tag{96}$$

then $w'' = 6w^2$, which is easily integrated yielding

$$(w')^2 = 4w^3 - g_3, \tag{97}$$

where g_3 is a constant.

The solution of this differential equation is the *Weierstrass function* $\wp(z; 0, g_3)$, since $\wp(z; g_2, g_3)$ verifies that $(\wp')^2 = 4\wp^3 - g_2\wp - g_3$. Hence, the solution of the Helmholtz oscillator with damping is $w = \wp(z; 0, g_3)$, which is called the *equianharmonic case of the Weierstrass function* because $g_2 = 0$ [39].

It should be noticed that $g_3 = 4w^3 - (w')^2$ is a first integral of motion and when a change of variables from (w, z) to (x, t) is carried out in Eq. (97), the first integral g_3 becomes $I(t, x, \dot{x})$ in this manner

$$\left[\left(\dot{x} + \frac{2}{5}\delta x\right)^2 - \frac{2}{3}\beta x^3\right] e^{\frac{6}{5}\delta t} = \Lambda g_3 = I(t, x, \dot{x}), \tag{98}$$

where $\Lambda = \left(\frac{6B^3\delta^3}{125\beta}\right)^2$, and consequently is always a positive constant.

The former result is an explicitely time-dependent first integral which is analogous to the first integral of the Duffing oscillator obtained in [62]. Also, it can be related to the Hamiltonian function of the Helmholtz oscillator with friction in the following way. Define two variables p and q as follows

$$p = \sqrt{2}\left(\dot{x} + \frac{2}{5}\delta x\right) e^{\frac{3}{5}\delta t}, \tag{99}$$

$$q = \sqrt{2} x e^{\frac{2}{5}\delta t}, \tag{100}$$

so the first integral $I(t, x, \dot{x})$ can be written as

$$I(p,q) = \frac{1}{2}p^2 - \frac{\beta}{3\sqrt{2}}q^3. \tag{101}$$

Define a function $H(p, q, t)$ related to the first integral $I(p, q)$ as

$$H(p,q,t) = I(p,q)e^{-\frac{1}{5}\delta t} = \left(\frac{1}{2}p^2 - \frac{\beta}{3\sqrt{2}}q^3\right)e^{-\frac{1}{5}\delta t}. \tag{102}$$

This function verifies the Hamilton equations, namely

$$\begin{aligned}\frac{\partial H}{\partial p} &= pe^{-\frac{1}{5}\delta t} = \sqrt{2}\left(\dot{x} + \frac{2}{5}\delta x\right)e^{\frac{2}{5}\delta t} = \dot{q},\\ \frac{\partial H}{\partial q} &= -\frac{\beta}{\sqrt{2}}q^2 e^{-\frac{1}{5}\delta t} = -\sqrt{2}\beta x^2 e^{\frac{3}{5}\delta t} = -\dot{p},\end{aligned} \tag{103}$$

and hence $H(p, q, t)$ is a Hamiltonian function. Moreover, by means of Eqs. (103) it is obtained that

$$\ddot{q} = \left(\dot{p} - \frac{1}{5}\delta p\right)e^{-\frac{1}{5}\delta t} = \frac{\beta}{\sqrt{2}}qe^{-\frac{2}{5}\delta t} - \frac{1}{5}\delta pe^{-\frac{1}{5}\delta t}, \tag{104}$$

which can be written in terms of (x, t) by using Eqs. (99, 100) as

$$\sqrt{2}e^{\frac{2}{5}\delta t}\left(\ddot{x} + \delta\dot{x} + \frac{6\delta^2}{25}x - \beta x^2\right) = 0. \tag{105}$$

Therefore, $H(p, q, t)$ is the Hamiltonian function of the Helmholtz oscillator with friction for the integrable case since the solutions to $\ddot{x} + \delta\dot{x} + \frac{6\delta^2}{25}x - \beta x^2 = 0$ and the solutions to the Hamilton equations of $H(p, q, t)$ are the same. Then, two remarks can be made. Firstly, the explicitly time-dependent Hamiltonian is not a first integral of motion, which is reasonable since the energy is not constant in this system because of the damping. Secondly, the first integral $I(p, q)$ can be seen as the energy of a particle in a potential $V(q) = -\frac{\beta}{3\sqrt{2}}q^3$ and thus, the Helmholtz oscillator can be regarded as a system with energy $I(p, q)$ at $t = 0$ which vanishes exponentially with time.

D. Solutions of the integrable case

1. Case $g_3 = 0$

The equation to solve is $(w')^2 = 4w^3$ whose solution is $w = (z - c')^{-2}$ with c' an arbitrary constant. The definitions of w and z and the relation in Eq. (96) implies that

$$x(t) = \frac{6\delta^2}{25\beta}\left(1 + c_2 e^{\frac{1}{5}\delta t}\right)^{-2}, \tag{106}$$

where c_2 is an arbitrary constant because c' is arbitrary.

2. Case $g_3 > 0$

The Weierstrass function $\wp(z; g_2, g_3)$ for $g_2 = 0$ and $g_3 > 0$ can be written in terms of the Jacobian Elliptic cosine cn [39] as

$$w(z) = r + H\frac{1 + \mathrm{cn}\left(2\sqrt{H}z + c_2; m\right)}{1 - \mathrm{cn}\left(2\sqrt{H}z + c_2; m\right)}, \tag{107}$$

with c_2 an arbitrary constant and where $m = \frac{2-\sqrt{3}}{4} \simeq 0.067$ and $H = \sqrt{3}r$ with $r = \sqrt[3]{\frac{g_3}{4}}$. Notice that, as it was explained in section II C, it is being used the elliptic parameter m instead of the elliptic modulus k, which are related in this way $k^2 = m$.

By using the definitions of w and z and the relation in Eq. (96) the following result in terms of t is obtained

$$x(t) = \frac{6\delta^2}{100\beta}c_1^2\left[\frac{1}{\sqrt{3}} + \frac{1 + \mathrm{cn}\left(c_1 e^{-\frac{1}{5}\delta t} + c_2; m\right)}{1 - \mathrm{cn}\left(c_1 e^{-\frac{1}{5}\delta t} + c_2; m\right)}\right] e^{-\frac{2}{5}\delta t}, \tag{108}$$

where $c_1 = 2\sqrt{H}B$ and hence c_1 is arbitrary because B is arbitrary.

3. Case $g_3 < 0$

It is known [39] that $\wp(z; g_2, g_3) = -\wp(iz; g_2, -g_3)$. This relation lets apply the result in Eq. (107) for $g_3 < 0$ this way

$$w(z) = -r' - H'\frac{1 + \mathrm{cn}\left(2\sqrt{H'}iz + ic_2; m\right)}{1 - \mathrm{cn}\left(2\sqrt{H'}iz + ic_2; m\right)}, \tag{109}$$

where $m = \frac{2-\sqrt{3}}{4}$ and $H' = \sqrt{3}r'$ with $r' = \sqrt[3]{\frac{|g_3|}{4}}$. By means of the relation $\mathrm{cn}(iu; m)\mathrm{cn}(u; m') = 1$ where $m + m' = 1$, it is possible to write Eq. (109) as follows

$$w(z) = -r' + H'\frac{1 + \mathrm{cn}\left(2\sqrt{H'}z + c_2; m'\right)}{1 - \mathrm{cn}\left(2\sqrt{H'}z + c_2; m'\right)}, \tag{110}$$

Hence, the solution may be written in terms of t by changing variables and using Eq. (96)

$$x(t) = \frac{6\delta^2}{100\beta}c_1^2\left[-\frac{1}{\sqrt{3}} + \frac{1+\mathrm{cn}\left(c_1 e^{-\frac{1}{5}\delta t}+c_2;m'\right)}{1-\mathrm{cn}\left(c_1 e^{-\frac{1}{5}\delta t}+c_2;m'\right)}\right]e^{-\frac{2}{5}\delta t}, \tag{111}$$

where $m' = \frac{2+\sqrt{3}}{4} \simeq 0.933$ and $c_1 = 2\sqrt{H'B}$ and hence c_1 is arbitrary because B is arbitrary.

4. Discussion

In Fig. 3 the two basins of attraction of the Helmholtz oscillator are depicted in the phase space. The grey region represents the set of initial conditions which end up in the attractor (0, 0). They correspond to bounded orbits in the phase space which asymptotically spiral inside the potential well. The white region is the set of initial conditions which correspond to unbounded orbits, i.e., tending to infinity. The boundary

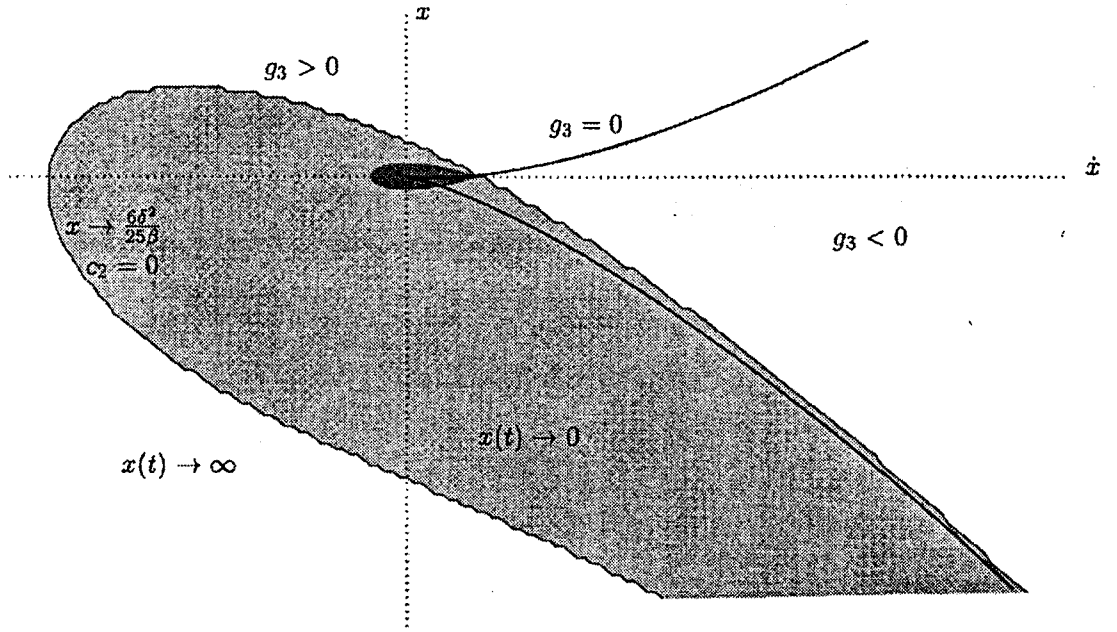

Figure 3. Relation between the geometry of the basins of attraction and the analytical features of the exact solutions when the Helmholtz oscillator is integrable. The grey region is made of the initial conditions which tend to (0, 0) and the white region is made of the ones tending to infinity. The boundary between both basins corresponds to the set of initial conditions tending to the local maximum and whose solutions have $c_2 = 0$. Also the curve $g_3 = 0$ is depicted and represents the initial conditions whose solutions have the first integral of motion $I(t, x, \dot{x}) = 0$. Finally, in dark grey is shown the region where there are bounded orbits in absence of damping. It is comparatively smaller than the region $x \to 0$ because the integrable case implies a large damping, since $\alpha = \frac{6}{25}\delta^2$, and hence dissipation makes more initial conditions end up inside the potential well.

between both sets is formed by the stable manifold of an unstable periodic orbit. Actually, this orbit is the one that stays forever on the local maximum $(\frac{6\delta^2}{25\beta}, 0)$ of the potential, which means that all points in the boundary tend asymptotically to this point.

The basins of attraction are related to the analytical solutions via c_2 and to check this, it is necessary to study the asymptotical behavior of the solutions. To calculate the limit $t \to \infty$ when $g_3 > 0$ the following change of variable $z \equiv c_1 e^{-\frac{1}{5}\delta t}$ is carried out, so the former limit becomes $z \to 0$. This implies in Eq. (107) that

$$\lim_{t\to\infty} x(t) = \lim_{z\to 0} \frac{6\delta^2}{100\beta}\left(\frac{1}{\sqrt{3}} + \frac{1+\mathrm{cn}(z+c_2;m)}{1-\mathrm{cn}(z+c_2;m)}\right) z^2. \tag{112}$$

It should be noticed that the Jacobian Elliptic function $\mathrm{cn}(z; m)$ is a periodic function since $\mathrm{cn}(z + 2K; m) = -\mathrm{cn}(z; m)$ i.e., $2K$ plays role similar to π in a circular function.In fact, cn is periodic with period $4K$ where $2K \simeq 3.197$ because $m = \frac{2-\sqrt{3}}{4}$, and thus c_2 is comprised within $(-2K, 2K)$. Consequently, if $c_2 = 4NK$ with $N \in \mathbb{Z}$ then

$$\begin{aligned}\lim_{t\to\infty} x(t) &= \lim_{z\to 0} \frac{6\delta^2}{100\beta}\left(\frac{1}{\sqrt{3}} + \frac{1+\mathrm{cn}(z;m)}{1-\mathrm{cn}(z;m)}\right) z^2 \\ &= \lim_{z\to 0} \frac{6\delta^2}{100\beta}\left(\frac{1}{\sqrt{3}} + \frac{4-z^2}{z^2}\right) z^2 = \frac{6\delta^2}{25\beta},\end{aligned} \tag{113}$$

where it has been used the following result $\mathrm{cn}(z; m) = 1 - \frac{1}{2}z^2 + o(z^4)$ [39]. Therefore, the boundary when $g_3 > 0$ can be defined to as the points in the phase space whose analytical solutions have $c_2 = 0$.

When $g_3 < 0$ the result $x(t \to \infty) = \frac{6\delta^2}{25\beta}$ when $c_2 = 0$ is equally achieved. However, now $\mathrm{cn}(z; m')$ is a periodic function with $2K' \simeq 5.535$ since $m' = \frac{2+\sqrt{3}}{4}$, and thus c_2 is comprised within $(-2K', 2K')$. Nevertheless, also in this case the boundary can be defined to as the points in the phase space whose analytical solutions have $c_2 = 0$. Also, it is easy to verify from Eq. (106) that in the case $g_3 = 0$ the solution tends to $\frac{6\delta^2}{25\beta}$ when $c_2 = 0$.

In summary, the condition $c_2 = 0$ on the exact solutions yields the boundary between the two basins of attraction, which links the geometry of these two regions in the phase space with an analytical feature in the exact solutions.

Inside the gray region in Fig. 3, it can be seen in black the region where there are bounded orbits in absence of damping. It is a small region as compared with the integrable case because $\alpha = \frac{6\delta^2}{25}$ and then, dissipation is more important than its potential energy. In other words, many initial conditions which were unbounded orbits without damping dissipate energy quickly in this case and, as they go by the potential well, are trapped in it.

The existence of a strong dissipation in the integrable case also explains why there is no oscillatory behavior in Fig. 4. When the orbit tends to the minimum inside the well the particle is so damped that it goes straight to that minimum.

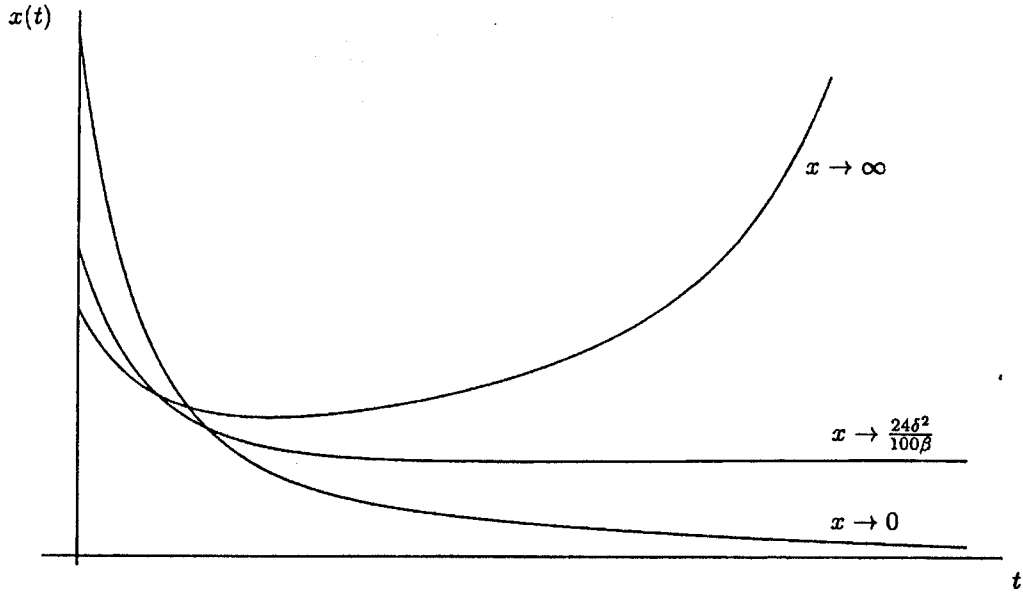

Figure 4. The phase space of the Helmholtz oscillator with friction has two basins of attraction and hence there are three kinds of orbits. Orbits spiralling inside the potential well tending to the minimum $x \to 0$, orbits tending to infinity $x \to \infty$ and orbits tending to the local maximum $x \to \frac{24\delta^2}{100\beta}$ which correspond to initial conditions upon the boundary of both basins. Notice that particles are so damped in the integrable case that inside the potential well they go straight to zero instead of spiralling and so there are no oscillations in the curve $x \to 0$.

V. Effect of the nonlinear damping

A. Introduction

Much of the discussion in the physics and engineering literature concerning damped oscillations, focuses on systems subject to viscous damping, that is, damping proportional to the velocity, even though viscous damping occurs rarely in physical systems. This is done mainly because the introduction of a linear term in the differential equation modelling the system makes easy its analysis.

Other types of dissipative forces, such as Coulomb damping or aerodynamic drag exist and are present in real systems. However, they are usually neglected, since their presence leads to nonlinear terms in the differential equation, making the system much more difficult to analyze. This is why in describing many oscillatory phenomena that occurs in nature, nonlinear oscillators with linear damping terms have been considered.

It is known also that frictional or drag forces which describe the motion of a object through a fluid or gas are rather complicated, and different phenomenological models have been proposed. One of the simplest empirical mathematical model is taken to be of the form $f(v) \propto v\,|v|^{p-1}$, where v represents the velocity of the object and p, a positive integer, the damping exponent.

Phenomenological models describing some type of nonlinear dissipation have been used in some applied sciences such as ship dynamics [63, 64], where a particular interest has deserved the role played by different damping mechanisms in the formulation of ship stability criteria, and vibration engineering (see [14, 15]).

Of special interest to our purposes is the comprehensive study on the effect of damping on basin and steady state bifurcation patterns of this oscillator, which is reported in [19]. In particular they investigated the effect of damping on the resonance response curves and how the main bifurcation boundaries, such as period-doubling bifurcation and boundary crisis, where the system escapes, are affected. (see [65] for a basic and rigorous description of boundary crises and the associated concept of transient chaos).

They also showed how the damping level affects the erosion of the non-escaping basin. Basically its main results are that, once the parameters of the system are fixed, a decrease in the damping level produces the effect of shifting backwards in parameter space the period-doubling bifurcation and the final boundary crisis leading to escape, destroying the safe basins and increasing the basin erosion patterns. As a consequence, it suggests the use of damping to suppress large scale erosion of the basin.

Nonlinear damping terms are of diverse nature and we choose here strictly dissipative nonlinear damping terms proportional to the pth power of velocity. Taking nonlinear damping terms of different damping exponent, we carry out a comprehensive study on how this affects the dynamics of the oscillator, the main bifurcations and the basin of attraction patterns when different periodic attractors may coexist prior to escape from the potential well.

The numerical results obtained show evidence that the period-doubling bifurcations and boundary crises leading to escape shift backwards in parameter space. An analytical study using Melnikov theory predicts rather well a shift of this kind in the computation and numerical observation of the appearance of the fractal basin boundaries [66, 67].

On the other hand different numerical experiments show that increasing the damping exponent strongly influences the erosion pattern of the basin. All these phenomena suggest that fixing parameters of the system and varying only the damping exponent p, taking positive integers, has similar effects as decreasing the damping level for the linear damping case.

B. The nonlinearly damped universal escape oscillator

In [19] it is studied with considerable detail the effects of the damping level on the resonance response of the steady state solutions and in the basin bifurcation patterns of the escape oscillator. In particular they analyzed the effect of using different damping levels and how this contributes to the erosion of the safe areas in phase space, and they also provide a comprehensive global picture of the main bifurcation boundaries.

If it is considered the same equation but including nonlinear damping terms as a power series on the velocity, the equation of motion reads

$$\ddot{x} + \sum_{p=1}^{n} \delta \dot{x} \, |\dot{x}|^{p-1} + \alpha x - \beta x^2 = F \sin(\omega t), \tag{114}$$

where δ is the damping level, p is the damping exponent, α and β define the potential and F and ω the forcing amplitude and the frequency of the external perturbation respectively.

However, for simplicity, only a single damping term proportional to the pth power of the velocity is taken, thus the equation to study is

$$\ddot{x} + \delta\dot{x}\,|\dot{x}|^{p-1} + x - x^2 = F\sin(\omega t), \tag{115}$$

where it is assumed that $\alpha = \beta = 1$ in order to emphasize the effect of the damping. A similar nonlinear damping term was used by [14, 15, 63].

As in [19], for most of the numerical computations it is used a fixed frequency $\omega = 0.85$ and a damping level $\delta = 0.1$ and when the damping exponent p is modified, it is observed that the basins erose strongly as the damping parameter p increases. The effect is similar to keeping fixed all parameters and decreasing the forcing term. For $p = 1$ and for the initial condition (0.175, –0.55), which is close to a fixed point attractor, a nice Feigenbaum period-doubling cascade in the forcing parameter range $0.1 \leq F \leq 0.109$ is found (this corresponds to the result shown in [2, 16]).

It is indicated in [19] that reducing the damping level, the period-doubling-escape scenario takes place at lower forcing amplitudes. In particular they studied the influence of modifying the forcing and damping level. When a quadratic nonlinear damping is used, that is $p = 2$, and for the same initial condition as before, a chaotic cascade in the parameter range $0.087 \leq F \leq 0.096$ appears, and which is shown in Fig. 5. One of the effects of using the quadratic nonlinear damping is precisely the lowering of the critical forcing for which the homoclinic bifurcation and the escape boundary take place. In particular for $F = 0.0954$, the result is a beautiful two piece chaotic attractor with a Lyapunov dimension $D_L = 1.22$.

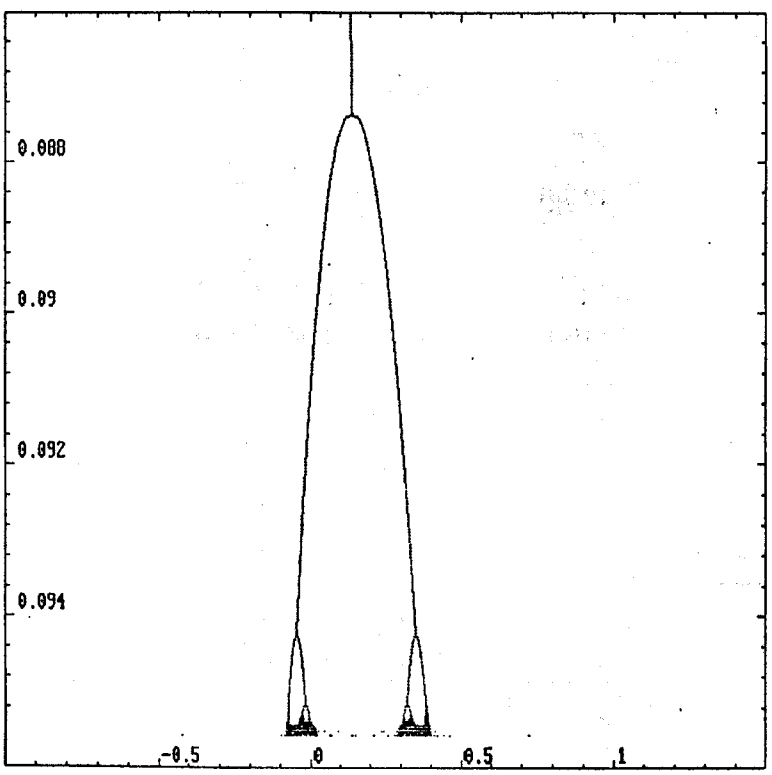

Figure 5. Plot of the period-doubling bifurcation diagram of the nonlinear escape oscillator with equation $\ddot{x} + 0.1\dot{x}\,|\dot{x}| + x - x^2 = F\sin 0.85t$ for the initial condition (0.175, – 0.55). The variation of the forcing amplitude is $0.086 < F < 0.096$.

When $p = 3$, that is a cubic nonlinear damping, chaotic solutions are found as well in the parameter region $0.083 \leq F \leq 0.093$. Consequently it appears to be a shift backwards in the period-doubling bifurcation threshold and escape as the damping exponent p is increased. If the numerical experiments are compared to the results shown for the linear damping case $p = 1$ in [19], we may conclude that increasing the damping exponent p has similar effects as decreasing the damping level δ.

There is a rather intuitive argument to justify this behavior. Think for simplicity in a particle moving with certain energy inside the potential well. Using topological arguments concerning the phase space of the escape oscillator, the velocity $\dot{x}(t)$ is bounded and $|\dot{x}(t)| < 1$ for all times, for any motion inside the potential well. This being so, it implies that $|\dot{x}(t)|^p < |\dot{x}(t)| < 1$, for $p > 1$. So this explains intuitively the observations of the numerical experiments carried out for different values of the damping exponent, since using a parameter $p > 1$ implies a reduction of the damping term which numerically is equivalent to using the linear damping term with a lower damping level.

C. Melnikov analysis for the nonlinear damping case

The numerical results given in the previous section suggest that when a nonlinear damping term is used instead of a linear damping term the global pattern of bifurcations is affected. The Melnikov analysis provides an analytical estimate of the parameters for which homoclinic bifurcations occur, and as it was proved by [66], the critical parameters derived from this analysis signal the appearance of fractal basin boundaries between coexisting attractors.

The aim now is to apply the Melnikov method to the nonlinearly damped and sinusoidally forced escape oscillator

$$\ddot{x} + \delta\dot{x}\,|\dot{x}|^{p-1} + x - x^2 = F\sin(\omega t), \tag{116}$$

where $p \geq 1$ is the damping exponent. From the Eqs. (30,31), it is easy to check that the equations of the separatrix orbit for the unperturbed system given by the Eq. (115) are

$$x_{sx}(t) = 1 - \frac{3}{2}\cosh^{-2}\left(\frac{t}{2}\right), \tag{117}$$

$$y_{sx}(t) = \frac{3\sinh\left(\frac{t}{2}\right)}{2\cosh^3\left(\frac{t}{2}\right)} \tag{118}$$

When the damping and the forcing are taken into account as a small perturbation to the unperturbed system, there is an associated Melnikov function which is given by

$$\Delta(t_0, \omega, p) = \int_{-\infty}^{+\infty} y_{sx}(t) F \sin\left[\omega(t + t_0)\right] dt - \int_{-\infty}^{+\infty} \delta y_{sx}^{p+1}(t) dt. \tag{119}$$

Thus the Melnikov function can be written as

$$\Delta(t_0,\omega,p)=\frac{3}{2}F\cos(\omega t_0)\int_{-\infty}^{+\infty}\frac{\sinh\left(\frac{t}{2}\right)}{\cosh^3\left(\frac{t}{2}\right)}\sin(\omega t)dt-\delta\int_{-\infty}^{+\infty}\left[\frac{3\sinh\left(\frac{t}{2}\right)}{2\cosh^3\left(\frac{t}{2}\right)}\right]^{p+1}dt, \quad (120)$$

which gives the following result

$$\Delta(t_0,\omega,p)=\frac{6\pi\omega^2F\cos(\omega t_0)}{\sinh(\pi\omega)}-2\delta\left(\frac{3}{2}\right)^{p+1}\mathcal{B}\left(\frac{p+2}{2},p+1\right), \quad (121)$$

where $\mathcal{B}(m,n)$ is the Euler Beta function, which can be easily evaluated in terms of the Euler Gamma function [39].

The critical forcing parameter F_{cp} for which homoclinic tangles intersect, that for a certain frequency ω depends on the damping exponent p and the damping coefficient δ, may be written as

$$F_{cp}=\delta\frac{\sinh(\pi\omega)}{3\pi\omega^2}\left(\frac{3}{2}\right)^{p+1}\mathcal{B}\left(\frac{p+2}{2},\frac{p+1}{2}\right). \quad (122)$$

When more nonlinear damping terms are considered, then the Melnikov function takes the form of

$$\Delta(t_0,\omega,p)=\frac{6\pi\omega^2F\cos(\omega t_0)}{\sinh(\pi\omega)}-\sum_{p=1}^{n}2\delta\left(\frac{3}{2}\right)^{p+1}\mathcal{B}\left(\frac{p+2}{2},p+1\right), \quad (123)$$

and consequently the critical parameter of the external perturbation is given by

$$F_{cp}=\sinh(\pi\omega)\sum_{p=1}^{n}\frac{\delta}{3\pi\omega^2}\left(\frac{3}{2}\right)^{p+1}\mathcal{B}\left(\frac{p+2}{2},\frac{p+1}{2}\right), \quad (124)$$

which gives an idea of the effect of the nonlinear damping terms on the threshold of homoclinic chaos and the associated appearance of fractal basin boundaries.

The Melnikov ratio $R(\omega,p)$ represents the ratio of the forcing to the damping level (F_{cp}/δ), which obviously depends on the frequency ω and the damping exponent p. According to Eq. (122) it takes the expression

$$R(\omega,p)=\frac{\sinh(\pi\omega)}{3\pi\omega^2}\left(\frac{3}{2}\right)^{p+1}\mathcal{B}\left(\frac{p+2}{2},\frac{p+1}{2}\right). \quad (125)$$

Fig. 6 depicts the variation of the Melnikov ratio $R(\omega,p)$ with the damping exponent p, which shows a decaying dependence on p. Hence when a nonlinear damping term is used instead of a linear damping term, with a fixed damping level δ, then the critical forcing for fractal basin boundaries to occur decreases.

In the case of linear damping, $p=1$, the Melnikov ratio is given by $R(\omega,1)=\sinh(\pi\omega)/5\pi\omega^2$ and the critical forcing, when $\omega=0.85$, is $F=0.633\delta$, which is the expression obtained by [2, 16].

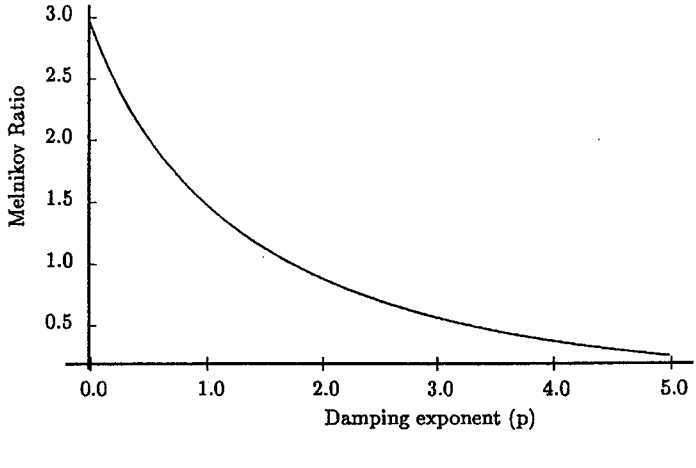

Figure 6. The Melnikov ratio $R(\omega,p) = F_{cp}/\delta$ versus the damping exponent p is plotted. Here is evidenced that for higher values of the damping exponent, the critical forcing necessary for the fractalization of the boundaries decreases.

The critical forcing terms for the quadratic and cubic nonlinear damping, with damping level $\delta = 0.1$, have been explicitly calculated. Its values are $F = 0.0297$ for the quadratic case and $F = 0.0148$ for the cubic case. As it was proved by [66], this critical forcing gives the threshold for the fractal basin boundaries. Moreover for this critical values the invariant manifolds associated to the fixed point of saddle type of the Poincaré map associated to the escape oscillator, intersect themselves tangentially.

Fig. 7(a) shows the tangency of the unstable (the inset) and stable (the outset) manifolds associated to the saddle fixed point situated at (0.999, –0.015), for $F = 0.0297$ and $\omega = 0.85$, with quadratic nonlinear damping. The homoclinic tangency for the invariant manifolds associated to the saddle fixed point at (0.999, –0.007) for $F = 0.0148$ and $\omega = 0.85$ is shown in Fig. 7(b), when a cubic nonlinear damping is considered. The inset is the unstable manifold and the outset is the stable manifold.

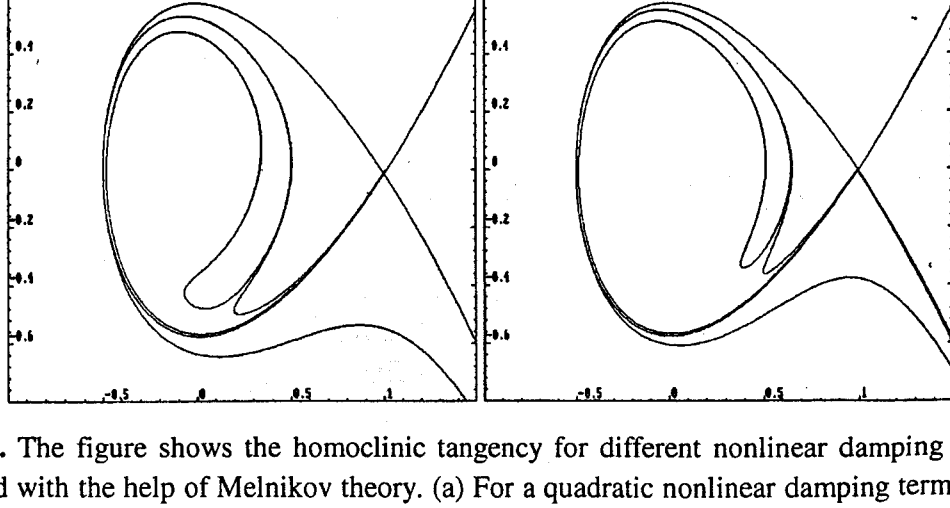

Figure 7. The figure shows the homoclinic tangency for different nonlinear damping terms, as calculated with the help of Melnikov theory. (a) For a quadratic nonlinear damping term, $p = 2$, $\beta = 0.1$, and $F = 0.0297$ (b) For a cubic nonlinear damping term, $p = 3$, $\beta = 0.1$, and $F = 0.0148$.

D. Basins of attraction

A basin of attraction is defined as the set of points that taken as initial conditions are attracted to a fixed point or an invariant set (see [65, 68]). As it was mentioned previously, the escape oscillator may be seen as a mechanical oscillator where a particle of unit mass moves inside an asymmetrical potential well, with the possibility of escape. This means that besides the possible attractors that may coexist in the interior of the well, the infinity may be taken as an attractor as well. The basin of attraction in this case signals the points in phase space that are attracted to a safe oscillation within the potential well, and the set of points that escape outside the potential well to the infinity.

A study of these basins of attraction for the escape oscillator was done extensively and with considerable detail by [2, 16-21]. Attention is focused here in especial to the paper by [19], where the effect of the damping level is analyzed. What we want to remark here is the effect of using nonlinear damping terms on the equation of the escape oscillator and how the basins of attraction are affected as the damping exponent p is increased.

We follow two strategies. The first one consists in fixing the forcing amplitude $F = 0.05$ and for three different sets of damping levels at $\delta = 0.1$, $\delta = 0.15$ and $\delta = 0.2$ for different damping exponents, that is, linear damping, quadratic damping and cubic damping, to compute the basins of attraction. To numerically generate the basins of attraction, a grid of 300×300 points is selected in the region of phase space determined by the rectangle of points $(-0.8, 1.4) \times (-0.8, 0.8)$, which are taken as initial conditions. Depending to which attractor an initial point goes, it is assigned a different color. Those initial points which go to any attractor located in the interior of the well are assigned the color white. The color black is assigned to any initial point which escapes the potential well.

These computations are shown in Fig. 8. The first column shows the basins of attraction for a fixed value of the damping level, $\delta = 0.1$, the second column corresponds to $\delta = 0.15$ and the third column to $\delta = 0.2$. On the other hand the first row corresponds to damping exponent $p = 1$, that is, linear damping, the second row to $p = 2$, quadratic nonlinear damping, and the third row to $p = 3$, cubic nonlinear damping. Observing these basins of attraction in Fig. 8 it is inferred that for a fixed damping level, the increase of the damping exponent, has a clear effect on the destruction of the safe areas inside the well and the erosion of the basins increases notably. If we compare these results to the corresponding results for linear damping for which only the damping level is varied, the conclusion is that they are equivalent to a decrease of the damping level.

The second strategy is fixing the damping level at $\delta = 0.1$ and considering different values of forcing amplitudes such as $F = 0.03$, $F = 0.05$ and $F = 0.07$ for the linear, quadratic and cubic dampings. The first column of Fig. 9 shows the basins of attraction for $F = 0.03$, the second column corresponds to $F = 0.05$ and the third column to $F = 0.07$. The rows correspond to linear, quadratic and cubic damping respectively.

The basins in this figure show that indeed the damping exponent has a strong effect on the erosion of the basin, but the strongest effect is manifested by the increase of the forcing as it happens as well in the linear damping case. Similar heuristic arguments as the ones given in the previous sections explain this behavior.

In some of these basins shown in Fig. 8 & Fig. 9 two attractors coexist in absence of any kind of fractalization of the boundaries. Something interesting to mention concerning most basins shown here is the presence of very clear basin cells [13, 68, 69].

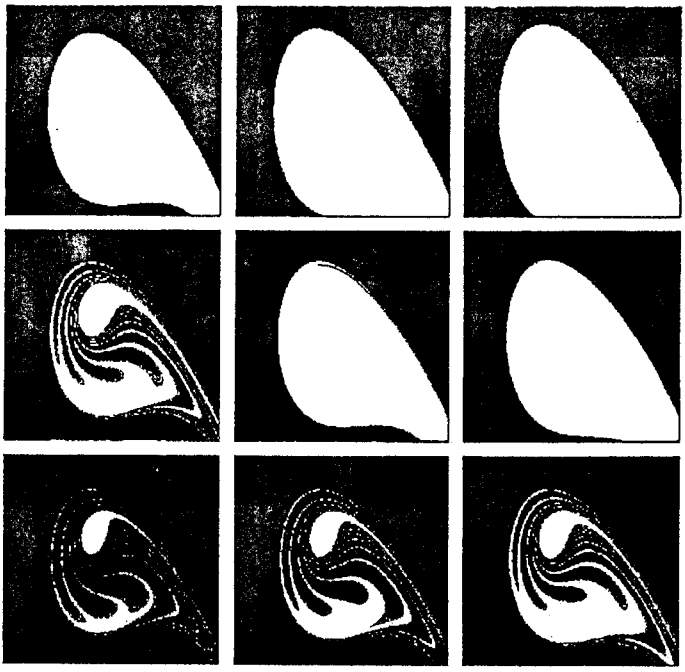

Figure 8. The figure shows the basin erosion pattern of the escape oscillator $\ddot{x} + \delta\dot{x}\,|\dot{x}|^{p-1} + x - x^2 = 0.05 \sin 0.85t$. The first column corresponds to a damping level $\delta = 0.1$, the second to $\delta = 0.15$, and the third one to $\delta = 0.2$. Different rows represent different damping exponents. The first row corresponds to $p = 1$, the second row to $p = 2$ and the third row to $p = 3$.

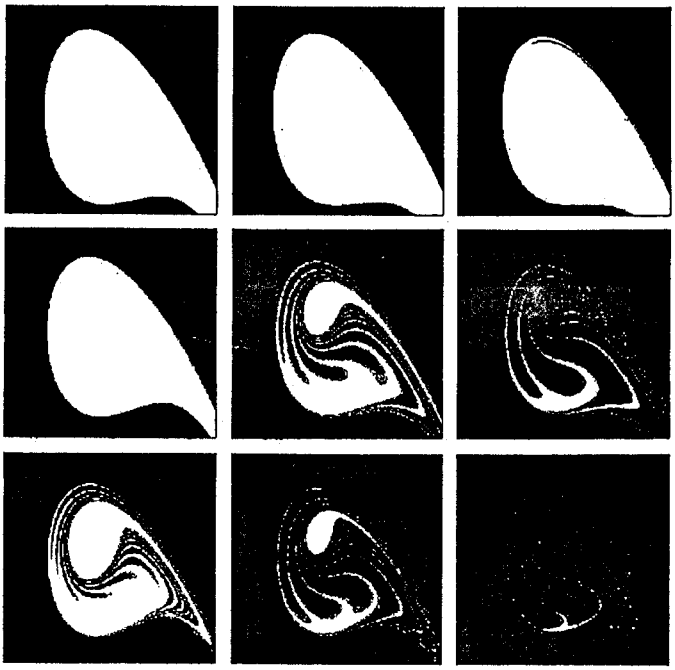

Figure 9. Basin erosion pattern of the escape oscillator $\ddot{x} + 0.1\dot{x}\,|\dot{x}|^{p-1} + x - x^2 = F \sin 0.85t$. The first column corresponds to a forcing amplitude $F = 0.03$, the second to $F = 0.05$, and the third one to $F = 0.07$. Concerning rows, the first row corresponds to $p = 1$, the second row to $p = 2$ and the third row to $p = 3$.

The notion of a trapping region clarifies this idea. A trapping region is a region in phase space from which points cannot escape. Once the trajectory enters the region cannot leave it and also there must be at least one attractor located there. A cell is a region in phase space whose boundary consists of pieces of the stable and unstable curves of some periodic trajectories. When a cell is a trapping region then is a basin cell. One of these basin cells is shown crosshatched in Fig. 10, and corresponds to $p = 3$, $\delta = 0.1$ and $F = 0.03$. A period 1 orbit which generates the basin cell, which is situated at the coordinates (0.092, 0.425) and the boundaries are its associated stable and unstable manifolds.

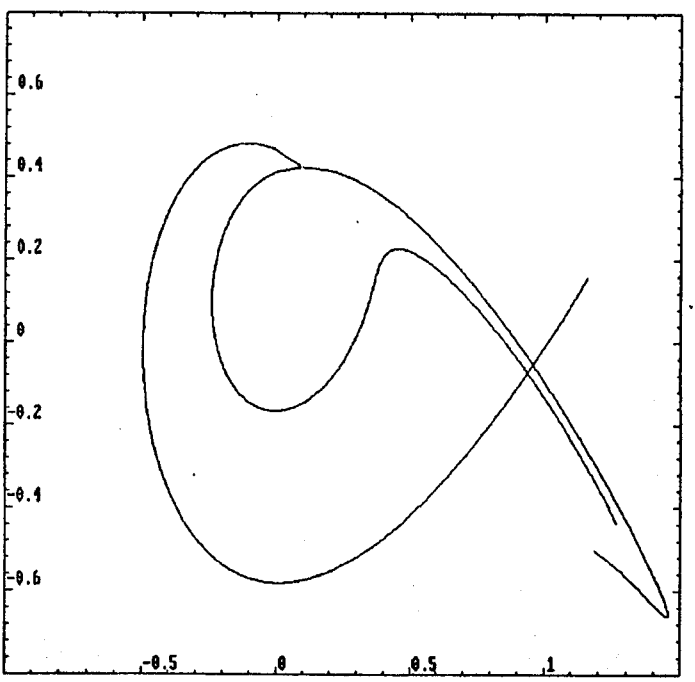

Figure 10. Basin cell, crosshatched, of the escape oscillator with equation $\ddot{x} + 0.1\dot{x}\,|\dot{x}|^2 + x - x^2 = 0.03 \sin 0.85t$ generated by a period 1 orbit situated at (0.092; 0.425).

VI. Concluding remarks

The Helmholtz oscillator is a simple model for studying phenomena which under certain conditions present a stable behavior of oscillatory kind, but for other conditions the behavior is unstable (i.e., this oscillator presents an escape). Then, a question of interest is what happens close to the separatrix when a forcing term is introduced. The effect of forcing is not relevant for an orbit with little energy (i.e., close to the minimum in the potential well), because essentially its stable behavior is not altered by the forcing. The width of the stochastic layer by using the separatrix map has been computed. This gives the width of the energy band around the separatrix, where it is likely that an orbit presents transient chaos.

We have shown that there exist two basic types of homoclinic bifurcation sets. If we have a quasiperiodically driven nonlinear oscillator, we obtain a bifurcation set from which a homoclinic bifurcation set as in [42] is derived. However, if we consider the

parametric drive of one component of the state variable, or both, along with the external forcing, the homoclinic bifurcation set for the nonlinear oscillator is similar to one in [56]. This is nothing strange, because the calculation of the bifurcation set depends directly on the computation of the Melnikov integral. For the quasiperiodically driven systems this integral involves integrands of the same nature. For the parametrically driven systems, the Melnikov integral involves terms of different nature, since the parametric terms involve the state variable.

Another important aspect considered in this paper is the inclusion of friction. To solve the equation of the Helmholtz oscillator with friction and without forcing the Lie theory for differential equations is used. We show that the Helmholtz oscillator is completely integrable only when certain relation between the parameters is satisfied. When this relation is not satisfied, the equation is partially integrable. Also, we calculate that the symmetries for the completely integrable case are a translation and a homothopy. Moreover, this two symmetries are the two dimensional algebra of the homothety transformations of the real line, and the symmetry for the partially integrable case is a translation.

A first integral of motion is obtained when the equation is integrated by using one symmetry. We prove that this time-dependent integral of motion is related to a Hamiltonian function. The second symmetry allows integrating the first integral of motion to obtain, as a solution, the Weierstrass function. Finally, we write this solution in terms of Jacobian Elliptic functions to show that there exists a relation with the basins of attraction of the oscillator.

We have analyzed the case of nonlinear dissipation in detail. We understand that, although the study of the effect of the damping level on the dynamics of the universal escape oscillator is interesting, this has to be extended to the case of nonlinear dissipation, because it is a natural extension to some phenomenological models. In particular we have analyzed by numerical methods, and also by using the analytical method provided by the Melnikov theory, how the introduction of nonlinear damping terms affects the threshold of the period-doubling bifurcation route to chaos, the boundary crises leading to final escape to infinity and the threshold parameter for the appearance of the fractal basin boundaries.

As a result, a good agreement between the analytical estimates and the numerical observations is observed. Moreover the effect of using different nonlinear damping terms on the erosion of the non-escaping basin has been studied. By fixing all the parameters of the system and varying only the damping exponent, the observation is that the increase of the damping exponent provokes a rapid erosion of the basin of attraction. When the damping level is increased a safe region increases, but it is rapidly eroded as the damping exponent also increases. Decreasing the forcing level for the linear damping case helps in the suppression of the erosion basin, but if at the same time the damping exponent is increased the situation is similar as if the forcing were increased. When the forcing is increased the erosion of the basin is bigger, and becomes even bigger if at the same time the damping exponent is increased. In the case of the linear damping and a fixed forcing, the erosion of the basin increases while the damping level is decreased, and a fixed value of the damping level the erosion is bigger when the forcing is increased. All this suggest that the increase of the damping exponent has similar effects as of decreasing the damping level for a linearly damped model.

Much work has been done on the study of this simple nonlinear oscillator, although it should not be thought that it is exhaustive. As a paradigm in nonlinear dynamics, the progress carried out on it, might be applied to analyze the different phenomena in nature that can be modeled by it. In this context it is possible to affirm that in spite of the work done, many aspects are still open for future research.

Acknowledegements

We acknowledge financial support from the Spanish Ministry of Science and Technology under projects BFM2000-0967 and BFM2003-03081 and from the Universidad Rey Juan Carlos under projects URJC-PIGE-02-04 and URJC-GCO-2003-16.

References

1. Rasband, S.N. 1987, Int. J. Non-Linear Mechanics, 22, 477.
2. Thompson, J.M. 1989, Proc. R. Soc. Lond. A., 421, 195.
3. Kang, I.S. and Leal, L.G. 1990, J. Fluid Mechanics, 218, 41.
4. Kang, I.S. 1993, J. Fluid Mechanics, 257, 229.
5. Bogdanova-Ryzhova, E.V. and Ryzhov, O.S. 1995, Phil. Trans. R. Soc. Lond. A, 352, 389.
6. Craik, A.D.D. 1985, Wave interactions and fluid flows, Cambridge University Press, Cambridge.
7. Grimshaw, R. and Tian, X. 1994, Proc. R. Soc. Lond. A, 445, 1.
8. Sanjuán, M.A.F. 1995, J. Sound and Vibration, 185, 734.
9. Zimmermann, W.B and Velarde, M.G. 1994, Nonlinear Proc. Geophysics, 1, 219.
10. Chirikov, B.V. 1979, Phys. Rep., 52, 263.
11. Zaslavsky, G.M., Sagdeev, R.Z., Usikov, D.A., and Chernikov, A.A. 1991, Weak Chaos and Quasi-regular Patterns, Cambridge University Press, Cambridge.
12. Yamaguchi, Y. 1985, Phys. Lett. A, 109, 191.
13. Nusse, H.E., Ott, E.,and Yorke, J.A. 1995, Phys. Rev. Lett., 75, 2482.
14. Ravindra, B. and Mallik, A.K. 1994, Phys. Rev. E, 49, 4950.
15. Ravindra, B. and Mallik, A.K. 1994, J. Sound and Vibration, 171, 708.
16. Thompson, J.M.T., Bishop, S.R., and Leung, L.M. 1987, Phys. Lett. A, 121, 116.
17. Thompson, J.M.T. 1990, Proc. Roy. Soc. Lond. A, 428, 1.
18. Soliman, M.S. and Thompson, J.M.T. 1991, Int. J. Bif. and Chaos, 1, 107.
19. Soliman, M.S. and Thompson, J.M.T. 1992, Int. J. Bif. and Chaos, 2, 81.
20. Stewart, H.B., Thompson, J.M.T., Lansbury, A.N., and Ueda, Y. 1991, Int. J. Bif. and Chaos, 1, 265.
21. Soliman, M.S. 1994, Int. J. Bif. and Chaos, 4, 1645.
22. Szemplińska-Stupnicka and Rudowski, J. 1996, Int. J. Non-Linear Mechanics, 31, 255.
23. Chacón, R., Balibrea, F., and López, M.A. 1997, Phys. Lett. A, 235, 153.
24. Sanjuán, M.A.F. 1996, Int. J. Th. Phys., 35, 1745.
25. Gottwald, J.A., Virgin, L.N., and Dowell, E.H. 1995, J. Sound and Vibrations, 187, 134.
26. Lenci, S., and Rega, G.2003, J. of Vibration and Control, 9, 281.
27. Almendral, J.A., and Sanjuán, M.A.F. 2003, J. of Physics A: Mathematics & General, 36, 695.
28. Sanjuán, M.A.F. 1998, Int. J. of Bifurcation ans Chaos, 9, 735.
29. Baltanás, J.P., Trueba, J.L., and Sanjuán, M.A.F. 2002, Recent Res. Devel. Sound & Vibration, 1, 29.
30. Nagem, R., Rhodes, B.A., and Sandri, G.V.H. 1991, J. Sound and Vibration, 144, 536.
31. Nagem, R.J. and Sandri, G.V.H. 1992, J. Sound and Vibration, 154, 552.
32. Rollins, D.K., and Shivamoggi B.K. 1992, J. Sound and Vibration, 154, 551.

33. Nagem, R.J. and Sandri, G.V.H. 1994, J. Sound and Vibration, 169, 270.
34. Bateman, H. 1931, Phys. Rev., 38, 815.
35. Pedrosa, I.A. 1987, J. Math. Phys., 28, 2662.
36. Havas, P. 1957, Nuovo Cimento., 3, 364.
37. Denman, H.H. and Buch, L.H. 1973, J. Math. Phys., 14, 326.
38. Steeb, W.H. and Kunick, A. 1982, Phys. Rev. A., 25, 2889.
39. Abramowitz, M. and Stegun, I.A. 1970, Handbook of Mathematical Functions, Dover, New York.
40. Zaslavsky, G. 1998, The Physics of Chaos in Hamiltonian Dynamics, Imperial College Press, London.
41. Moon, F.C. 1992, Chaotic and Fractal Dynamics, Wiley, New York.
42. Ide, K. and Wiggins, S. 1989, Physica D, 34, 169.
43. Parthasarathy, S. and Lakshmanan, M. 1990, J. Sound and Vibration, 137, 523.
44. McLaughlin, J.B. 1981, J. Stat. Phys., 24, 375.
45. Koch, B.P. and Leven, R.W. 1985, Physica D, 16, 1.
46. Wiggins, S. 1987, Phys. Lett. A, 124, 138.
47. Lima, R. and Pettini, M. 1990, Phys. Rev. A., 41, 726.
48. Yagasaki, K. 1992, SIAM J. Math. Anal., 23, 1230.
49. Kapitaniak, T. 1993, Phys. Rev. E, 47, 1408.
50. Cicogna, G. and Fronzoni, L. 1993, Phys. Rev. E., 47, 4585.
51. Cuadros, F. and Chacon, R. 1993, Phys. Rev. E., 47, 4628.
52. Kivshar, Y., Rodelspeger, F., and Benner, H. 1994, Phys. Rev. E., 49, 319.
53. Wiggins, S. 1990, Introduction to Applied Nonlinear Dynamical Systems and Chaos, Springer-Verlag, Berlin.
54. Lima, R. and Pettini, M. 1993, Phys. Rev. E., 47, 4630.
55. Grauer, R., Spatschek, K.H., and Zolotaryuk, A.V. 1993, Phys. Rev. E., 47, 236.
56. Parthasarathy, S. 1992, Phys. Rev. A., 46, 2147.
57. Tabor, M. 1984, Nature, 310, 277.
58. Giacomini, H. and Neukirch, S. 1997, Phys. Lett. A., 277, 309.
59. Chang, Y.T., Tabor, M., and Weiss, J. 1982, J. Math. Phys., 23, 531.
60. Ibragimov, N.H. 1994, Lie group analysis of differential equations Vol.1, CRC Press, Boca Raton.
61. Olver, P.J. 2000, Applications of Lie Groups to differential equations, Springer, New York.
62. Euler, N., Steeb, W.H., and Cyrus, K. 1989, J. Phys. A., 22, 195.
63. Bikdash, M., Balachandran, B., and Nayfeh, A. 1994, Nonlinear Dynamics, 6, 101.
64. Falzarano, J.M., Shaw, S.W., and Troesch, A.W. 1992, Int. J. Bif. and Chaos, 2, 101.
65. Alligood, K.T., Sauer, T.D., and Yorke, J.A. 1997, Chaos: An Introduction to Dynamical Systems, Springer, New York.
66. Moon, F.C. and Li, G.X. 1985, Phys. Rev. Lett., 55, 1439.
67. Mcdonald, S.W., Grebogi, C., Ott, E., and Yorke, J.A. 1985, Physica D, 17, 125.
68. Nusse, H.E., and Yorke, J.A. 1996, Science, 271, 1376.
69. Nusse, H.E., and Yorke, J.A. 1996, Physica D, 90, 242.